Available online at www.sciencedirect.com
SCIENCE DIRECT®
Physica D 189 (2004) 247–276
PHYSICA D
www.elsevier.com/locate/physd

Bifurcations in systems with Z_2 spatio-temporal and O(2) spatial symmetry

F. Marques [a,*], J.M. Lopez [b], H.M. Blackburn [c]

[a] *Departament de Física Aplicada, Universitat Politècnica de Catalunya, Girona Salgado s/n, Mòdul B4 Campus Nord, 08034 Barcelona, Spain*
[b] *Department of Mathematics and Statistics, Arizona State University, Tempe, AZ 85287-1804, USA*
[c] *CSIRO Manufacturing and Infrastructure Technology, P.O. Box 56, Highett, Vic. 3190, Australia*

Received 23 June 2003; accepted 27 September 2003
Communicated by S. Fauve

Abstract

This work analyzes the O(2) symmetry breaking bifurcations in systems with an $Z_2 \times O(2)$ symmetry group—where Z_2 and O(2) are, respectively, spatio-temporal and spatial symmetries—that are responsible for the transitions from two-dimensional to three-dimensional hydrodynamic states. This symmetry group describes, for example, two-dimensional time-periodic flows past bodies which have reflection symmetry across a wake center plane, such as symmetrical airfoils, circular and square cylinders. Normal form analysis of these systems is based on a joint representation of the monodromy matrix for the half-period-flip map (a composition of a half-period temporal evolution with a spatial reflection) and the spatial O(2) symmetry. There are exactly two kinds of codimension-one synchronous bifurcations in these systems; one preserves the Z_2 spatio-temporal symmetry, while the other breaks it. When the Floquet multipliers occur in complex-conjugate pairs (non-resonant with the periodic basic state), there is a single codimension-one bifurcation, and at the bifurcation point two different kind of solutions appear simultaneously: a pair of modulated traveling waves, and a circle of modulated standing waves. At most one of these two types has stable solutions. The symmetries of the system also admit period-doubling bifurcations, but these are codimension-two and the normal form analysis permits specific conclusions regarding these. There are also a number of other codimension-two bifurcations leading to mixed modes and the strong 1:1 and 1:2 resonances. All the codimension-one bifurcations are illustrated with reference to a concrete physical example.

Keywords: Symmetry breaking; Floquet analysis; Normal forms

1. Introduction

The transition from two-dimensional to three-dimensional flows in hydrodynamics is a fundamental step towards turbulence. There are numerous situations where the two-dimensional state is also time-periodic and has symmetries additional to the invariance in the third dimension (usually referred to as the spanwise direction). A

* Corresponding author.
E-mail address: marques@fa.upc.es (F. Marques).

0167-2789/$ – see front matter © 2003 Elsevier B.V. All rights reserved.
doi:10.1016/j.physd.2003.09.041

classic example is the two-dimensional periodically shedding wake of a bluff body, such as a circular cylinder, i.e. the well-known von Kármán vortex street. The transition from two-dimensional to three-dimensional flow is a breaking of the O(2) symmetry in the spanwise direction, whereby the three-dimensional state has spatially periodic structure in the spanwise direction and constitutes a breaking of the spanwise translation invariance component of the O(2) symmetry. However, in this class of flows, it is not sufficient to consider just O(2) symmetry breaking, as there are additional spatio-temporal symmetries that have important consequences for the symmetry breaking process.

Spatio-temporal symmetry breaking has been considered in many contexts for time-periodic symmetric systems, e.g. see [6–10]. The usual way to investigate the stability of time-periodic flows is to analyze the corresponding Poincaré map, but in many time-periodic symmetric systems, the Poincaré map is the nth iterate of another map that mixes a spatial symmetry (typically a reflection) with time evolution. Swift and Wiesenfeld [18] considered the simplest such spatio-temporal symmetry, consisting of a half-period temporal evolution composed with a spatial reflection, and proved that this symmetry inhibits period doubling. These ideas have been generalized (e.g. [14]), and the dynamic consequences of this type of spatio-temporal symmetry have been explored in diverse circumstances (e.g. [11,17]).

These studies have focused on the implications imposed on the dynamics solely by the spatio-temporal symmetry, whereas in the class of problems we wish to address, one must also consider the implications of the spanwise O(2) symmetry. This requires the consideration of the joint action of the O(2) and the spatio-temporal symmetries.

In this paper, we first derive the joint representations of the spanwise O(2) symmetry and the spatially orthogonal (e.g. streamwise) spatio-temporal symmetry. Following this, the corresponding normal forms are derived in center manifolds of low dimension and where the action of the O(2) symmetry is non-trivial—we are primarily interested in the transition from two-dimensional to three-dimensional flows, and the cases where O(2) acts trivially have essentially been treated in the studies of the spatio-temporal symmetry alone. The dynamics of the normal forms, corresponding to codimension-one bifurcations to three-dimensional flows, are analyzed and compared to nonlinear results (both computational and experimental) of a physical hydrodynamics example, which we detail in the following section.

2. Periodically driven cavity flow

As an example to illustrate the general theory presented in this paper, we use the periodically driven cavity flow, which we briefly describe here and refer the reader to [4,19] for further details, including experimental observations, numerical Floquet analysis and numerical nonlinear computations. This flow provides examples of all possible codimension-one local bifurcations from the basic state leading to three-dimensional flows.

The flow is confined in a rectangular cavity, as shown in Fig. 1(a), and is driven by the harmonic oscillations of the wall at $x = 0$, with period T. The x-extent of the cavity, h, is used as the length scale. The other stationary cavity walls are at $x = h$ and $y = \pm\Gamma h/2$, where Γ is the aspect ratio. The basic state is invariant in the spanwise z-direction, and is also invariant to the spatio-temporal symmetry $\mathcal{H}$, consisting of a spatial y-reflection, K_y, composed with a temporal evolution through half the forcing period, T, as illustrated in Fig. 1(b). For three-dimensional flows we assume z-periodicity with wave number β.

The equations and boundary conditions of the problem are

$$\text{Navier–Stokes}: \quad \partial_t \boldsymbol{u} + \boldsymbol{u}\cdot\boldsymbol{\nabla}\boldsymbol{u} = -\rho^{-1}\nabla p + \nu\Delta\boldsymbol{u}, \tag{1}$$

$$\text{incompressibility}: \quad \nabla\cdot\boldsymbol{u} = 0, \tag{2}$$

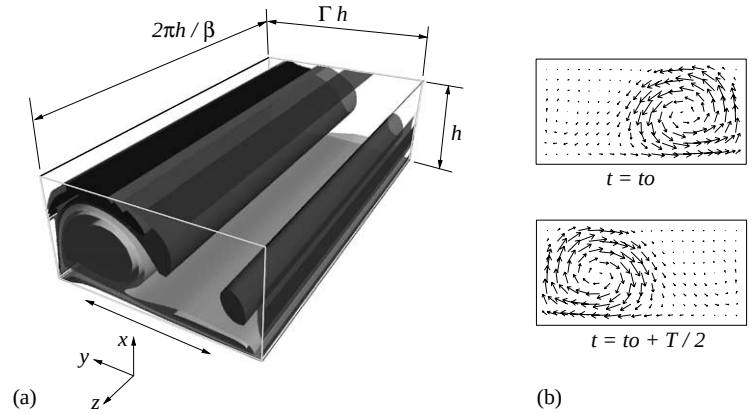

Fig. 1. (a) Schematic of the fluid domain for the periodically driven cavity flow, periodic in the z-direction and forced in the y-direction, with isosurfaces representing different values of spanwise vorticity. (b) Two snapshots of velocity vectors of the base flow, half a forcing period apart, illustrating its spatio-temporal symmetry.

$$\text{boundary conditions}: \quad \begin{cases} \boldsymbol{u}\left(x, y, -\dfrac{\pi h}{\beta}, t\right) = \boldsymbol{u}\left(x, y, \dfrac{\pi h}{\beta}, t\right), \\ \boldsymbol{u}\left(x, -\dfrac{\Gamma h}{2}, z, t\right) = 0, \\ \boldsymbol{u}\left(x, \dfrac{\Gamma h}{2}, z, t\right) = 0, \\ \boldsymbol{u}(h, y, z, t) = 0, \\ \boldsymbol{u}(0, y, z, t) = \left(0, V_{\max} \sin\left(\dfrac{2\pi t}{T}\right), 0\right), \end{cases} \tag{3}$$

where (u, v, w) are the physical components of the velocity in Cartesian coordinates $(x, y, z) \in [0, h] \times [-\Gamma h/2, \Gamma h/2] \times [-\pi h/\beta, \pi h/\beta]$. These equations and boundary conditions are invariant to the following spatial symmetries:

$$z\text{-translation}: \quad R_\alpha(u, v, w)(x, y, z, t) = (u, v, w)(x, y, z + \alpha, t), \tag{4}$$

$$z\text{-reflection}: \quad K_z(u, v, w)(x, y, z, t) = (u, v, -w)(x, y, -z, t). \tag{5}$$

Reflection in y, K_y, acts on a velocity field as

$$y\text{-reflection}: \quad K_y(u, v, w)(x, y, z, t) = (u, -v, w)(x, -y, z, t). \tag{6}$$

K_y is not a symmetry of the system, due to the periodic forcing in the y-direction, but is part of the spatio-temporal symmetry $\mathcal{H}$:

$$\mathcal{H}\text{-symmetry}: \quad \mathcal{H}(u, v, w)(x, y, z, t) = (u, -v, w)(x, -y, z, t + \tfrac{1}{2}T). \tag{7}$$

R_α generates the group SO(2), and K_z generates a group Z_2, but R_α and K_z do not commute: $R_\alpha K_z = K_z R_{-\alpha}$. The symmetry group generated by R_α and K_z is O(2), acting in the periodic spanwise z-direction. The transformation K_y generates another Z_2 group and commutes with the spanwise O(2). The complete symmetry group of the problem is $Z_2 \times \mathrm{O}(2)$.

The action of the spatio-temporal symmetry $\mathcal{H}$ on the vorticity, $\nabla \times \boldsymbol{u} = (\xi, \eta, \zeta)$, is different to the action of $\mathcal{H}$ on the velocity, and is given by

$$\mathcal{H}\text{-symmetry}: \quad \mathcal{H}(\xi, \eta, \zeta)(x, y, z, t) = (-\xi, \eta, -\zeta)(x, -y, z, t + \tfrac{1}{2}T). \tag{8}$$

Physically, the two-dimensional basic state of the flow is generated by oscillatory Stokes layers that are produced through the simple harmonic motion of the cavity wall at $x = 0$, and their containment by the stationary walls. The basic state has spanwise 'rollers', as illustrated by the vorticity isosurfaces and velocity vectors of Fig. 1. Three dimensionless parameters govern the flow: the Reynolds number $Re = V_{\max} h/\nu$ and the Stokes number $St = h^2/T\nu$ (measuring the amplitude and period of the floor motion), and the aspect ratio Γ. The flow shares many physical features with two-dimensional time-periodic bluff body wakes, and in fact is equivariant to the same symmetry group.

In different regions of parameter space, the two-dimensional basic state (a $Z_2 \times \mathrm{O}(2)$-invariant limit cycle), loses stability to three-dimensional perturbations in three distinct ways, leading to modes A, B and QP. The three modes break the SO(2) group generated by R_α. They differ in their time dependence (periodic or quasi-periodic), and in the way they break the remaining symmetries $\mathcal{H}$ and K_z. Modes A and B are *synchronous* limit cycles—therefore the critical Floquet multiplier of the Poincaré map is real—with long and short spanwise wavelengths, respectively, and which bear similarities to the cylinder wake modes of the same names. Mode QP is a *quasi-periodic* solution, with complex-conjugate pair critical Floquet multipliers.

3. Bifurcations with a Z_2 spatio-temporal symmetry

Let us consider a non-autonomous ODE in a finite-dimensional linear space E, of the form:

$$\dot{x} = f(x, t), \qquad f(x, t + T) = f(x, t) \quad \forall t \in \mathbb{R}, \quad x \in E, \tag{9}$$

representing our T-periodically forced system. Let K be a linear transformation in E representing the spatio-temporal symmetry $\mathcal{H}$ of our problem, such that

$$\mathcal{H} f(x, t) = K f(Kx, t + \tfrac{1}{2}T) = f(x, t), \quad K^2 = I. \tag{10}$$

$K = K_y$ in the periodically driven cavity flow. The vector field $f(x, t)$ is defined in $\tilde{E} = E \times S^1$, the enhanced phase space of our problem, with coordinates (x, t); S^1 is the unit circle on which t is identified with $t + T$. The ODE (9) becomes an autonomous ODE in $\tilde{E}$ in a natural way by augmenting the ODE with the equation $\dot{t} = 1$. A global Poincaré map is defined by advancing any given initial condition, x_0, a period T in time:

$$\mathcal{P} : E_{t_0} \mapsto E_{t_0}, \qquad x_0 \mapsto \mathcal{P}x_0 = \phi(t_0 + T; x_0, t_0), \tag{11}$$

where $\phi(t; x_0, t_0)$ is the solution of (9) at a time t corresponding to the initial condition x_0 at $t = t_0$:

$$\partial_t \phi(t; x_0, t_0) = f(\phi(t; x_0, t_0), t), \quad \phi(t_0; x_0, t_0) = x_0. \tag{12}$$

E_{t_0} is the section of $\tilde{E}$ at an arbitrary given time t_0 at which the Poincaré section is computed. In this ODE setting, all E_{t_0} coincide with E. Strictly speaking, the function $f(x, t)$ is defined in an open subset $\mathcal{U} \subset \tilde{E}$, and the restrictions of $\mathcal{U}$ to each E_{t_0}, $\mathcal{U}_{t_0}$, can be different, as illustrated in Fig. 2. If our dynamical system comes from a PDE, then E is infinite-dimensional. For example, if the dynamical system is the Navier–Stokes equations, with time-periodic boundary conditions, then the space E is the space of square-integrable solenoidal velocity fields (a Hilbert space). Since the boundary conditions may be different for different t_0-values, $\mathcal{U}_{t_0}$ is the subspace of E satisfying the boundary conditions of the problem *at* t_0.

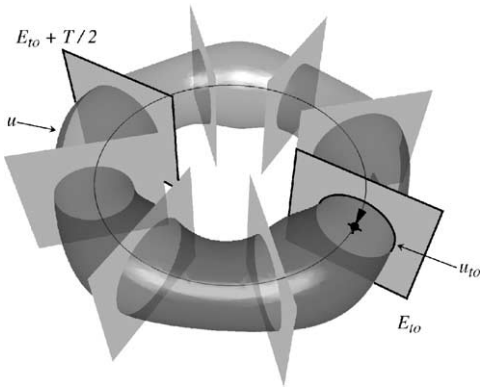

Fig. 2. Schematic of the enhanced phase space $\tilde{E} = E \times S^1$.

The analysis of periodic solutions of (9) reduces to the analysis of fixed points of $\mathcal{P}$. A spatio-temporal symmetry $\mathcal{H}$ does not fit into the standard framework of normal form analysis of equivariant differential equations because it mixes space and time, whereas the usual equivariant normal form theory has been developed for purely spatial symmetry transformations. For systems with a spatio-temporal symmetry $\mathcal{H}$, it is convenient to analyze the action of $\mathcal{H}$ at a given initial time t_0:

$$\mathcal{H} : E_{t_0} \mapsto E_{t_0}, \qquad x_0 \mapsto \mathcal{H}x_0 = K\phi(t_0 + \tfrac{1}{2}T; x_0, t_0). \tag{13}$$

The Poincaré map $\mathcal{P}$ is the square of the half-period-flip map $\mathcal{H}$.

Typically, the given ODE (9) will have symmetries additional to $\mathcal{H}$. Let us assume that (9) is equivariant to the symmetry group $\mathcal{G}$, whose elements are linear transformations in E:

$$Gf(x, t) = f(Gx, t) \quad \forall G \in \mathcal{G}. \tag{14}$$

$\mathcal{G}$ is the group of *spatial* symmetries. The complete group of symmetries of the ODE (9) is generated by $\mathcal{G}$ and K. If they commute, the group is $\Sigma = \mathcal{G} \times Z_2$; if not, it may be the semidirect product $\Sigma = \mathcal{G} \rtimes Z_2$, or it may have a more complex structure. In any case, Z_2 is generated by K and it only has two elements, $Z_2 = \{I, K\}$.

The Poincaré map $\mathcal{P}$ is $\mathcal{G}$-equivariant, i.e. it commutes with $\mathcal{G} : G\mathcal{P}x = \mathcal{P}Gx$, for all $G \in \mathcal{G}$. In general, $\mathcal{H}$ is not $\mathcal{G}$-equivariant, but satisfies

$$\mathcal{H}Gx = (KGK^{-1})\mathcal{H}x \quad \forall G \in \mathcal{G}, \ \ \forall x \in E_{t_0}. \tag{15}$$

When $\mathcal{H}$ is not $\mathcal{G}$-equivariant, it is called a *twisted equivariant* map, or a *k-symmetric* map. In [13,14], k is defined to be the least positive integer such that K^k commutes with all the elements in $\mathcal{G}$. Since $K^2 = I$ in our case, we either have $k = 1$ (and $\mathcal{H}$ is $\mathcal{G}$-equivariant), or $k = 2$ (and $\mathcal{H}$ is a 2-symmetric map). Therefore, $\mathcal{H}$ is $\mathcal{G}$-equivariant iff K commutes with $\mathcal{G}$; in this case, $\Sigma = \mathcal{G} \times Z_2$. In the driven cavity flow problem, $\mathcal{H}$ commutes with $\mathcal{G}$, $\Sigma = \mathcal{G} \times Z_2$ and $\mathcal{H}$ is not a twisted equivariant map, because $k = 1$.

In addition to the periodically forced cavity flow problem, periodic orbits with spatio-temporal symmetries are common in many unforced hydrodynamic systems with symmetry following a Hopf bifurcation. The use of the half-period-flip map is not only useful for periodically forced systems, but it can also be applied to autonomous system with periodic solutions, when the periodic solution considered has a spatio-temporal symmetry. Examples are bluff body wakes, Bénard convection and Taylor–Couette flows. The important point is that the bifurcations from these periodic solutions are governed by exactly the same normal forms both in forced and unforced systems.

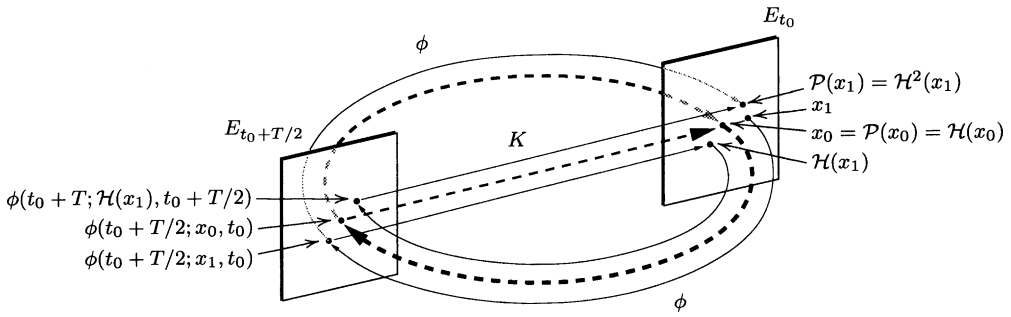

Fig. 3. The T-periodic Poincaré return map $\mathcal{P}$ and the half-period-flip map $\mathcal{H}$. The basic state (on dashed-line limit cycle) is x_0, a fixed point of $\mathcal{P}$ and $\mathcal{H}$; x_1 is an arbitrary initial point, close to x_0; x_1, $\mathcal{P}(x_1)$ and $\mathcal{H}(x_1)$ are all different, although $\mathcal{P}(x_1) = \mathcal{H}^2(x_1)$.

Consider an autonomous ODE in a finite-dimensional space E, of the form $\dot{y} = g(y)$, with a T-periodic solution $\phi_0(t, y_0) = \phi_0(t + T, y_0)$, where y_0 is any point of the periodic solution. Assume that this periodic solution is invariant to a Z_2 spatio-temporal symmetry:

$$\mathcal{H}\phi_0(t, y_0) = K\phi_0(t + \tfrac{1}{2}T, y_0) = \phi_0(t, y_0), \tag{16}$$

where K is a linear transformation in E representing the spatio-temporal symmetry of our problem, such that $K^2 = I$ and $g(Kx) = Kg(x)$; we are assuming that K is a symmetry of the ODE, but this symmetry is broken in the periodic solution ϕ_0, which only retains the spatio-temporal symmetry $\mathcal{H}$. Replacing y with $\phi_0(t, y_0) + x$ in the original ODE results in a new ODE:

$$\dot{x} = f(x, t), \qquad f(x, t + T) = f(x, t) \quad \forall t \in \mathbb{R}, \quad x \in E \tag{17}$$

which is a non-autonomous periodic ODE exactly of the same type as (9), and in particular $f(Kx, t+T/2) = Kf(x, t)$.

The analysis of the periodic solution $\phi_0(t, y_0)$ reduces to the analysis of the fixed point $x_0 = 0$ of the Poincaré map $\mathcal{P}$ or of the half-period-flip map $\mathcal{H}$, and we have reverted to the previous problem. If x_0 is a point of the periodic orbit of (9) or (17), it is a fixed point of both $\mathcal{P}$ and $\mathcal{H}$. The actions of $\mathcal{P}$ and $\mathcal{H}$ on points neighboring x_0 are illustrated in Fig. 3.

For the rest of this paper, we focus on the case $\mathcal{G} = \mathrm{O}(2)$ and $\Sigma = \mathrm{O}(2) \times Z_2$; these are the symmetries of the driven cavity flow, bluff body wakes, and other fluid dynamical systems.

4. Joint representations of O(2) and L_H

The center manifolds, $\mathcal{M}_c$, associated with the Poincaré map $\mathcal{P}$ and the half-period-flip map $\mathcal{H}$ are the same [14]. The eigenvalues and eigenvectors/eigenfunctions at a bifurcation point are computed by Floquet analysis of the governing equations linearized about the basic state. Since $\mathcal{P} = \mathcal{H}^2$, the monodromy matrix of $\mathcal{P}$, L_P, is the square of the monodromy matrix of $\mathcal{H}$, L_H : $L_P = L_H^2$. Both linear operators L_P and L_H act on E_c, the tangent space of the center manifold $\mathcal{M}_c$ at the basic state. Let μ_P and μ_H be the eigenvalues (Floquet multipliers) of L_P and L_H, respectively; then $\mu_P = \mu_H^2$, and the (generalized) eigenvectors are the same. As the governing equations are O(2)-equivariant, $\mathcal{M}_c$ is an O(2)-invariant manifold, and we seek the possible representations of O(2) in E_c. But $\mathcal{H}$ is also a symmetry of the problem, therefore we want to find the *joint representations* of O(2) and L_H in E_c, i.e. the matrix representations of the actions of these symmetries on a basis for E_c. From them, the corresponding analysis for L_P and $\mathcal{P}$ is immediate, and in addition, we gain a better understanding of the symmetry breaking process, because the spatio-temporal symmetry is built into the definition of $\mathcal{H}$.

The irreducible representations[1] of O(2) are either one-dimensional (and the action of SO(2), translations in z, is trivial) or two-dimensional. Any representation of O(2) in E_c is a direct sum of irreducible representations, and E_c splits into two invariant subspaces, $E_c = W_1 \oplus W_2$, where W_1 contains the one-dimensional irreducible components and W_2 contains the two-dimensional irreducible components of the representation considered [9]. SO(2) acts trivially on W_1, and the corresponding eigenvectors are SO(2)-invariant, i.e. they are independent of z. The action of SO(2) in W_2 is non-trivial, and any eigenvector in W_2 breaks the translational invariance in z. W_2 is even dimensional, and splits into a direct sum of two-dimensional irreducible representations. In a convenient complex basis, $\{\boldsymbol{U}, \bar{\boldsymbol{U}}\}$, the action of a two-dimensional irreducible representation of O(2) on the corresponding complex amplitudes $(A, \bar{A})$ is

$$R_\alpha = \begin{pmatrix} e^{i\beta\alpha} & 0 \\ 0 & e^{-i\beta\alpha} \end{pmatrix}, \qquad K_z = \begin{pmatrix} 0 & 1 \\ 1 & 0 \end{pmatrix}, \tag{18}$$

where $\beta = 2\pi/\lambda$ is the wavenumber of the eigenvector $\boldsymbol{U}$ in the spanwise direction.

As L_H commutes with O(2), W_1 and W_2 are L_H-invariant subspaces, and the joint representations of O(2) and L_H split into a direct sum of representations in W_1 and W_2 (see [9, Theorem 3.5]). As we are interested in the transitions to three-dimensional flows, i.e. SO(2) symmetry breaking bifurcations, we now derive the joint representations of O(2) and L_H in W_2. As W_2 is even, we present the results for the two-dimensional and four-dimensional cases.

4.1. Two-dimensional center manifold

As the representation of O(2) on E_c is irreducible, L_H must be a multiple of the identity because it commutes with O(2), and that multiple, μ_H, must be real as L_H stems from a real dynamical system. Furthermore, at the bifurcation, $|\mu_H| = 1$, and so there are *exactly* two different two-dimensional joint representations of O(2) and L_H, $\mathcal{F}_2^+$ and $\mathcal{F}_2^-$, corresponding to $\mu_H = 1$ and $\mu_H = -1$, respectively:

$$\mathcal{F}_2^+: \quad R_\alpha = \begin{pmatrix} e^{i\beta\alpha} & 0 \\ 0 & e^{-i\beta\alpha} \end{pmatrix}, \qquad K_z = \begin{pmatrix} 0 & 1 \\ 1 & 0 \end{pmatrix}, \qquad L_H = \begin{pmatrix} 1 & 0 \\ 0 & 1 \end{pmatrix}, \tag{19}$$

$$\mathcal{F}_2^-: \quad R_\alpha = \begin{pmatrix} e^{i\beta\alpha} & 0 \\ 0 & e^{-i\beta\alpha} \end{pmatrix}, \qquad K_z = \begin{pmatrix} 0 & 1 \\ 1 & 0 \end{pmatrix}, \qquad L_H = \begin{pmatrix} -1 & 0 \\ 0 & -1 \end{pmatrix}. \tag{20}$$

Both representations have the same L_P matrix, the identity $\mathbf{1}$. Although L_P is always the identity map, we have two different possibilities for L_H, either $\mathbf{1}$ or $-\mathbf{1}$. In the first case, the eigenvectors preserve the spatio-temporal symmetry $\mathcal{H}$, and in the second case, this symmetry is broken. This result is transparent from the map $\mathcal{H}$, but it is not obvious from the Poincaré map $\mathcal{P}$. Note that the two-dimensional representations account only for real eigenvalues of L_H (and L_P); in order to accommodate complex-conjugate eigenvalues (i.e. Neimark–Sacker bifurcations, Hopf bifurcations for maps) the center manifold $\mathcal{M}_c$ must be at least four-dimensional.

An important consequence of the joint representations found, is that period doubling in the Poincaré map $\mathcal{P}$ is inhibited when $\mathcal{M}_c$ is two-dimensional, even though the multipliers have multiplicity 2. This is an extension of the result of [18] to bifurcations with O(2) symmetry in addition to a spatio-temporal symmetry $\mathcal{H}$. If the system only had SO(2) symmetry instead of O(2) symmetry, then L_P and L_H would not be restricted to being proportional to

[1] A representation of a group in a linear space V is irreducible when its only invariant subspaces are the null space $\{0\}$ and the whole space V. Further, it is *absolutely* irreducible if the only linear operators commuting with the representation are multiples of the identity. Complex irreducible finite-dimensional representations are absolutely irreducible.

the identity and period doubling would be possible when $\mathcal{M}_c$ is two-dimensional. For example, L_P and L_H could have forms ($L_H^2 = L_P$):

$$\begin{pmatrix} \mathrm{i} & 0 \\ 0 & -\mathrm{i} \end{pmatrix}^2 = \begin{pmatrix} -1 & 0 \\ 0 & -1 \end{pmatrix} \quad \text{or} \quad \begin{pmatrix} 0 & -1 \\ 1 & 0 \end{pmatrix}^2 = \begin{pmatrix} -1 & 0 \\ 0 & -1 \end{pmatrix}. \tag{21}$$

When $\mathcal{M}_c$ is two-dimensional, E_c is K_z-invariant. In fact, any real solution $\boldsymbol{u}_0 = \exp(\mathrm{i}\gamma)\boldsymbol{U} + \exp(-\mathrm{i}\gamma)\bar{\boldsymbol{U}}$ in E_c is invariant to a z-reflection centered not about the origin $z = 0$, but about an appropriate $z = \gamma/\beta$:

$$(R_{\gamma/\beta} K_z R_{-\gamma/\beta})\boldsymbol{u}_0 = \boldsymbol{u}_0. \tag{22}$$

We say that the symmetry K_z is preserved in the two-dimensional joint representations $\mathcal{F}_2^+$ and $\mathcal{F}_2^-$ ($\mathcal{F}_2^s$, $s = \pm$).

4.2. Four-dimensional center manifold

Let us now consider the case where the center manifold $\mathcal{M}_c$ is four-dimensional. The representation of O(2) in E_c splits into two irreducible representations of the form (18) and we have five possibilities for the joint representations of O(2) and L_H in E_c; the details can be found in Appendix A. Two of these representations are new, and the other three are constructed using $\mathcal{F}_2^s$ as building blocks. These latter compound representations are the direct sums $\mathcal{F}_2^+ \oplus \mathcal{F}_2^+$, $\mathcal{F}_2^+ \oplus \mathcal{F}_2^-$ and $\mathcal{F}_2^- \oplus \mathcal{F}_2^-$, in which the value of β (the wave number in the spanwise direction) need not be the same in both elements of the direct sum. These essentially represent mixed modes.

The two new representations are

$$\mathcal{F}_4^c: \quad R_\alpha = \begin{pmatrix} \mathrm{e}^{\mathrm{i}\beta\alpha} & 0 & 0 & 0 \\ 0 & \mathrm{e}^{-\mathrm{i}\beta\alpha} & 0 & 0 \\ 0 & 0 & \mathrm{e}^{-\mathrm{i}\beta\alpha} & 0 \\ 0 & 0 & 0 & \mathrm{e}^{\mathrm{i}\beta\alpha} \end{pmatrix}, \qquad K_z = \begin{pmatrix} 0 & 1 & 0 & 0 \\ 1 & 0 & 0 & 0 \\ 0 & 0 & 0 & 1 \\ 0 & 0 & 1 & 0 \end{pmatrix},$$
$$L_H = \begin{pmatrix} \mu_H & 0 & 0 & 0 \\ 0 & \mu_H & 0 & 0 \\ 0 & 0 & \bar{\mu}_H & 0 \\ 0 & 0 & 0 & \bar{\mu}_H \end{pmatrix}, \tag{23}$$

$$\mathcal{F}_4^s: \quad R_\alpha = \begin{pmatrix} \mathrm{e}^{\mathrm{i}\beta\alpha} & 0 & 0 & 0 \\ 0 & \mathrm{e}^{\mathrm{i}\beta\alpha} & 0 & 0 \\ 0 & 0 & \mathrm{e}^{-\mathrm{i}\beta\alpha} & 0 \\ 0 & 0 & 0 & \mathrm{e}^{-\mathrm{i}\beta\alpha} \end{pmatrix}, \qquad K_z = \begin{pmatrix} 0 & 0 & 1 & 0 \\ 0 & 0 & 0 & 1 \\ 1 & 0 & 0 & 0 \\ 0 & 1 & 0 & 0 \end{pmatrix},$$
$$L_H = \begin{pmatrix} s & \delta_H & 0 & 0 \\ 0 & s & 0 & 0 \\ 0 & 0 & s & \delta_H \\ 0 & 0 & 0 & s \end{pmatrix}, \tag{24}$$

where $s = \pm 1$, μ_H is a complex number with $|\mu_H| = 1$ and $\mathrm{Im}(\mu_H) \neq 0$, and δ_H is any non-zero real number, usually 1, or a value that simplifies L_P. The basis associated with these representations is of the form $A\boldsymbol{U} + B\boldsymbol{V} + \bar{A}\bar{\boldsymbol{U}} + \bar{B}\bar{\boldsymbol{V}}$, and the matrices are the action of the symmetry operators on $(A, B, \bar{A}, \bar{B})$. In fact, there are two *families* of

four-dimensional representations, one ($\mathcal{F}_4^c$) parameterized by the *complex* number $\mu_H = e^{i\theta/2}$, with $\theta \in (0, 2\pi)$, and the other ($\mathcal{F}_4^s$) parameterized by the *sign* $s = \pm 1$.

The map L_H does not have any restriction, and depending on the system studied, any of the possibilities in (23) and (24) can occur. The Poincaré map L_P however, being the square of L_H, has only the following options, obtained by squaring the matrices of L_H in (23) and (24):

$$L_P = \begin{pmatrix} \mu_P & 0 & 0 & 0 \\ 0 & \mu_P & 0 & 0 \\ 0 & 0 & \overline{\mu}_P & 0 \\ 0 & 0 & 0 & \overline{\mu}_P \end{pmatrix} \quad \text{and} \quad L_P = \begin{pmatrix} 1 & \delta_P & 0 & 0 \\ 0 & 1 & 0 & 0 \\ 0 & 0 & 1 & \delta_P \\ 0 & 0 & 0 & 1 \end{pmatrix} \tag{25}$$

for the cases $\mathcal{F}_4^c$ and $\mathcal{F}_4^s$, respectively, where $\mu_P = \mu_H^2$, $\delta_P = 2s\delta_H$, and usually $\delta_P = 1$ so that $\delta_H = s/2$.

Period doubling in the Poincaré map L_P is now possible; we may have $\mu_P = -1$ in (25) by taking $\mu_H = i = e^{i\pi/2}$ in (23). So, if we have O(2) symmetry and the action of SO(2) is non-trivial, the center manifold $\mathcal{M}_c$ must be at least four-dimensional for period doubling to be possible.

5. Normal forms

The details of the derivation of the normal forms are given in Appendix B, and follows the method of [10].

5.1. Normal form for $\mathcal{F}_2^+$: $\mathcal{H}$-invariant synchronous bifurcation

Let us consider the joint representation $\mathcal{F}_2^+$ (19) in a two-dimensional center manifold. The linear part of $\mathcal{H}$ in the center manifold, parameterized by the amplitudes $(A, \bar{A})$, is $L_H = \mathbf{1}$. The normal form for $\mathcal{H}$ is (Appendix B.1):

$$A \mapsto A[1 + P(|A|^2, \varepsilon)], \tag{26}$$

where the polynomial P is real. Up to third order in A, we obtain the codimension-one normal form (where the signs of ε and $\tilde{a}$ have been chosen for convenience):

$$\mathcal{H}: \quad A \mapsto A(1 + \tilde{\varepsilon} - \tilde{a}|A|^2), \quad \tilde{a} \in \mathbb{R}. \tag{27}$$

This normal form is typical of the pitchfork bifurcation, except that here A is complex. The fixed points of $\mathcal{H}$ are the basic state $A = 0$, which is unstable for $\tilde{\varepsilon} > 0$, and an invariant circle of bifurcated fixed points:

$$A_\theta = e^{i\theta} \left(\frac{\tilde{\varepsilon}}{\tilde{a}}\right)^{1/2}, \quad \theta \in [0, 2\pi), \quad \frac{\tilde{\varepsilon}}{\tilde{a}} \geq 0, \tag{28}$$

parameterized by the angle θ, that exists for $\tilde{\varepsilon}/\tilde{a} > 0$. This is a pitchfork of revolution. The action of all the symmetries on these bifurcated solutions is

$$R_\alpha A_\theta = e^{i\beta\alpha} A_\theta = A_{\theta+\beta\alpha}, \qquad K_z A_\theta = A_{-\theta}, \qquad \mathcal{H} A_\theta = A_\theta. \tag{29}$$

The SO(2) symmetry is broken, and R_α transforms a solution on the invariant circle into a different solution on the same invariant circle. The two solutions A_0 and A_π are K_z-invariant, and in fact $R_{\theta/\beta} K_z R_{-\theta/\beta} A_\theta = A_\theta$; this means that A_θ is invariant to a z-reflection centered not about the origin, $z = 0$, but about $z = \theta/\beta$. We say that the K_z symmetry is preserved. The spatio-temporal symmetry $\mathcal{H}$ is also retained.

The $\mathcal{H}$-symmetric synchronous instability mode of the periodically driven cavity, mode B, is illustrated in Fig. 4, which shows vorticity isosurfaces at two instants, $T/2$ apart. The figure shows the saturated periodic state at *Re*

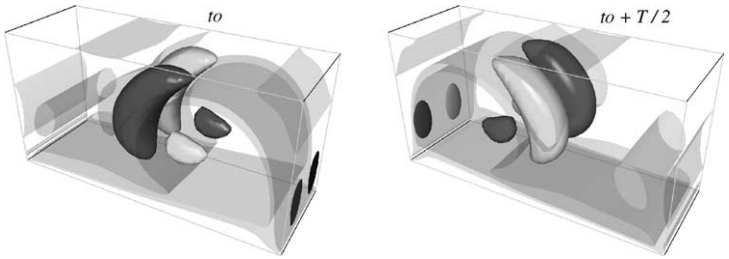

Fig. 4. Isosurfaces of the x-component (solid) and z-component (translucent) of vorticity for the $\mathcal{F}_2^+$ (synchronous, $\mathcal{H}$-symmetric) mode B of the periodically driven cavity flow, at $St = 20$, $Re = 535$, $\beta = 8.75$. This Re is slightly above critical for the value of St and the spanwise wavenumber is the critical value at the bifurcation. The plots are at two phases in the oscillation of the floor: t_0 and $t_0 + T/2$.

slightly above Re_c for the given value of $St = 20$, and the spanwise wavenumber β corresponds to the critical value at the bifurcation. Contours of perturbation eigenfunction velocity components for this state are shown in Fig. 5. By inspection of the eigenfunction velocity components, we see that mode B is $\mathcal{H}$-symmetric (7), and so at the bifurcation $\mu_H = +1$ for this mode. This can also be seen in Fig. 4, using the action of $\mathcal{H}$ on the vorticity (8).

The normal form corresponding to the Poincaré map is obtained by squaring that of $\mathcal{H}$, and has exactly the same form as the normal form for $\mathcal{H}$:

$$\mathcal{P} : A \mapsto A(1 + \varepsilon - a|A|^2), \quad \varepsilon = 2\tilde{\varepsilon}, \quad a = 2\tilde{a}. \tag{30}$$

As a readily computable measure of the perturbation amplitude A, we employ the square root of the normalized instantaneous kinetic energy in the first spanwise Fourier mode, $\boldsymbol{u}_1$, at times $t_0 + nT$ during the nonlinear evolution of the perturbed flow, i.e.

$$E_n = \left[\frac{1}{4V_{\max}^2 \Gamma h^2 \lambda} \int_0^h \int_{-\Gamma h/2}^{\Gamma h/2} \int_{-\lambda h/2}^{\lambda h/2} \boldsymbol{u}_1 \cdot \bar{\boldsymbol{u}}_1(t_0 + nT)\, \mathrm{d}z\, \mathrm{d}y\, \mathrm{d}x \right]^{1/2}. \tag{31}$$

Fig. 6 shows the nonlinear growth of E_n for the mode B instability of the periodically driven cavity flow at ($St = 20$, $Re = 535$), where $\varepsilon = 0.0600$. The observed growth fits very well to the normal form expression for $\mathcal{P}$, and from the saturation value E_n as $n \to \infty$, i.e. E_∞, we have $a = 7.45 \times 10^3 V_{\max}^{-2}$.

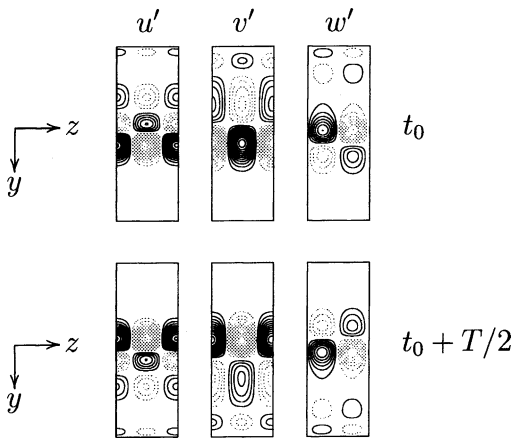

Fig. 5. Contours of the critical eigenfunction velocity components for the $\mathcal{F}_2^+$ mode B of the periodically driven rectangular cavity, plotted in the mid-depth plane at $x = h/2$; $y \in [-h, h]$ (vertical extent), $z \in [-\pi/\beta_c, \pi/\beta_c]$ (horizontal extent). Black (gray) contours represent positive (negative) values. Parameters values are $St = 20$, $Re_c = 532.5$ and $\beta_c = 8.75$.

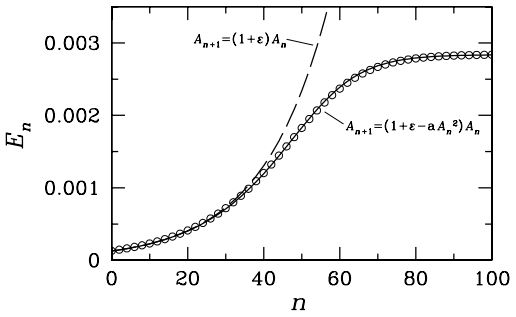

Fig. 6. Nonlinear growth of a measure of perturbation amplitude for the mode B instability of the periodically driven cavity at ($St = 20$, $Re = 535$). In order to avoid clutter, only every third cycle is represented.

The measure shown in Fig. 7, which is related to the mean squared saturation amplitude $\langle A_\infty^2 \rangle$ (and $\langle E_\infty^2 \rangle$):

$$q_z = \frac{1}{4V_{\max}^2 \Gamma h^2 \lambda} \int_0^h \int_{-\Gamma h/2}^{\Gamma h/2} \int_{-\lambda h/2}^{\lambda h/2} \langle w^2 \rangle \, \mathrm{d}z \, \mathrm{d}y \, \mathrm{d}x \tag{32}$$

is the normalized contribution to the time-averaged kinetic energy from the spanwise velocity component, which is zero for the base state. (The time-averaged value is used because in later examples, w^2, and E_n^2, have oscillatory behavior.) As expected for a supercritical pitchfork bifurcation, the growth of q_z with $|Re - Re_c|$ is linear.

5.2. Normal form for $\mathcal{F}_2^-$: synchronous bifurcation breaking the $\mathcal{H}$ symmetry

Let us consider the joint representation $\mathcal{F}_2^-$ (20) in a two-dimensional center manifold. The linear part of $\mathcal{H}$ in the center manifold is $L_H = -\mathbf{1}$, and the normal form for $\mathcal{H}$ is (Appendix B.1):

$$A \mapsto A[-1 + P(|A|^2, \varepsilon)] \tag{33}$$

with P a real polynomial. The normal form of $\mathcal{H}$ up to third order in A is

$$\mathcal{H} : A \mapsto A(-1 - \tilde{\varepsilon} + \tilde{a}|A|^2), \quad \tilde{a} \in \mathbb{R}, \ \ \tilde{a} \neq 0 \tag{34}$$

which is the normal form typical of period-doubling bifurcations, except that here A is complex. The only fixed point, $\mathcal{H}A = A$, is the basic state $A = 0$, which is unstable for $\tilde{\varepsilon} > 0$. The period-two points are the solutions of

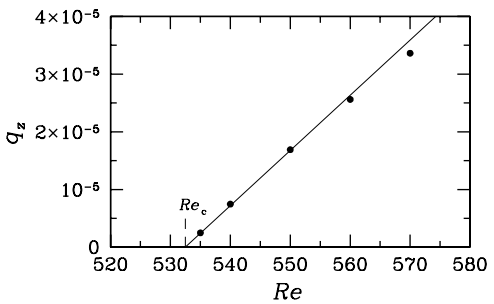

Fig. 7. Analysis of the growth in energy of the saturated perturbation flow, q_z, with departure from the critical Reynolds number $Re_c = 532.5$ at $St = 20$ for mode B of the cavity flow.

$\mathcal{H}A = -A$:

$$A_\theta = \mathrm{e}^{\mathrm{i}\theta}\left(\frac{\tilde{\varepsilon}}{\tilde{a}}\right)^{1/2}, \quad \theta \in [0, 2\pi), \quad \frac{\tilde{\varepsilon}}{\tilde{a}} \geq 0,$$

the same expression as in (28). For $\tilde{\varepsilon}/\tilde{a} > 0$ we have an invariant circle of period-two bifurcated solutions, parameterized by the angle θ (note that a period-two point of $\mathcal{H}$ has a period equal to that of the forcing period, T). The actions of all the symmetries on these bifurcated solutions are

$$R_\alpha A_\theta = \mathrm{e}^{\mathrm{i}\beta\alpha} A_\theta = A_{\theta+\beta\alpha}, \qquad K_z A_\theta = A_{-\theta}, \qquad \mathcal{H}A_\theta = -A_\theta = R_{\pi/\beta} A_\theta. \tag{35}$$

The SO(2) symmetry is broken and K_z is preserved, as in the $\mathcal{F}_2^+$ case. In the $\mathcal{F}_2^+$ case the eigenvector is $\mathcal{H}$-symmetric, as is the basic state. Therefore, the full solution of the problem (basic state plus perturbation) is also $\mathcal{H}$-symmetric. However, in the $\mathcal{F}_2^-$ case, applying $\mathcal{H}$ to the eigenvector results in the same eigenvector with the sign changed (a kind of anti-symmetry). The full solution of the problem, being the sum of the $\mathcal{H}$-symmetric basic state plus the (anti-symmetric) perturbation, does not exhibit a simple behavior under the $\mathcal{H}$-symmetry. We simply say that the $\mathcal{H}$-symmetry is broken. Nevertheless, the system retains a spatio-temporal symmetry, the transformation $\mathcal{H}$ composed with $R_{\pi/\beta}$: $R_{\pi/\beta}\mathcal{H}A_\theta = A_\theta$. Both $\mathcal{H}$ and $R_{\pi/\beta}$ symmetries are broken, but their combination is still a spatio-temporal symmetry: a half-wavelength translation in the spanwise direction z plus a reflection in y together with a $T/2$ temporal evolution.

All the bifurcated solutions for $\mathcal{F}_2^-$ period double on the half-period-flip map, but since the period of $\mathcal{H}$ is $T/2$, they have the same period as the forcing, T, and so are synchronous bifurcations of the Poincaré map. The normal form corresponding to the Poincaré map is obtained by squaring that of $\mathcal{H}$, and keeping terms up to third order in A and first order in $\tilde{\varepsilon}$ gives

$$\mathcal{P} : A \mapsto A(1 + \varepsilon - a|A|^2), \quad \varepsilon = 2\tilde{\varepsilon}, \quad a = 2\tilde{a}. \tag{36}$$

The bifurcated solutions now form an invariant circle of fixed points for $\mathcal{P}$, it is a pitchfork of revolution. R_α and $\mathcal{H}$ symmetries are broken, and K_z is preserved. All that remains of R_α and $\mathcal{H}$ is a single spatio-temporal symmetry, $R_{\pi/\beta}\mathcal{H}$, that generates a Z_2 group.

The normal forms corresponding to the Poincaré map for $\mathcal{F}_2^+$ and $\mathcal{F}_2^-$ cases are exactly the same (36). The essential difference between both cases is that $\mathcal{F}_2^+$ preserves the spatio-temporal symmetry $\mathcal{H}$ and $\mathcal{F}_2^-$ breaks it. That the two have different spatio-temporal symmetries is clearly evident from the normal forms of the half-period-flip map $\mathcal{H}$, but is completely hidden in the normal form of $\mathcal{P}$.

The $\mathcal{F}_2^-$ mode of the periodically driven cavity, mode A, is illustrated in Fig. 8, which shows vorticity isosurfaces at two instants, $T/2$ apart. The figure shows the saturated periodic state at *Re* slightly above Re_c for the given value

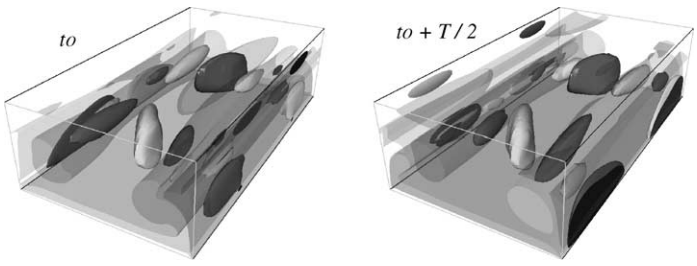

Fig. 8. Isosurfaces of the x-component (solid) and z-component (translucent) of vorticity for the $\mathcal{F}_2^-$ (synchronous, $\mathcal{H}$-symmetry breaking) mode A of the periodically driven cavity flow, at $St = 160$, $Re = 1250$, $\beta = 1.7$. This *Re* is slightly above critical for the value of *St* and the spanwise wavenumber is the critical value at the bifurcation. The plots are at two phases in the oscillation of the floor: t_0 and $t_0 + T/2$.

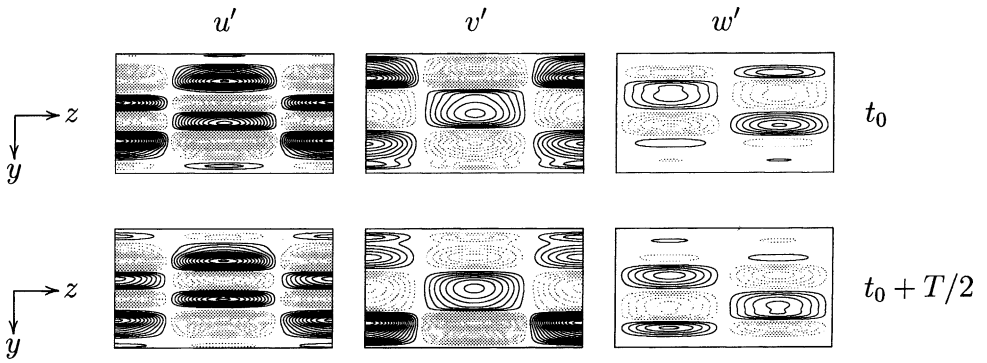

Fig. 9. Contours of the critical eigenfunction velocity components for the $\mathcal{F}_2^-$ mode A of the periodically driven rectangular cavity, plotted in the mid-depth plane at $x = h/2$; $y \in [-h, h]$ (vertical extent), $z \in [-\pi/\beta_c, \pi/\beta_c]$ (horizontal extent). Black (gray) contours represent positive (negative) values. Parameters values are $St = 160$, $Re_c = 1191$ and $\beta_c = 1.7$.

of $St = 160$, and the spanwise wavenumber β corresponds to the critical value at the bifurcation. Contours of perturbation eigenfunction velocity components for this state are shown in Fig. 9. By inspection, the eigenfunction velocity components for this mode A break $\mathcal{H}$-symmetry (7), and so at the bifurcation $\mu_H = -1$. This can also be seen in Fig. 8, using the action of $\mathcal{H}$ on the vorticity (8).

In the driven cavity flow, the long wavelength mode A is of $\mathcal{F}_2^-$ type and the short wavelength mode B is of $\mathcal{F}_2^+$ type. In contrast, for the wake flows the opposite is true; the long wavelength mode A is of $\mathcal{F}_2^+$ type and the short wavelength mode B is of $\mathcal{F}_2^-$ type [1–3,5,16].

In the driven cavity flow case, the nonlinear growth of the perturbation amplitude for the mode A instability does not follow the expression obtained from the normal form (36), because in this particular example we are very close to a degenerate case, where the coefficient a is very small. We now consider this degenerate case separately.

5.2.1. Normal form for $\mathcal{F}_2^-$: degenerate case

In the driven cavity flow, the coefficient $\tilde{a}$ of $|A|^2$ in (34) is very close to zero, so the bifurcation is degenerate, and we must keep terms to fifth order in the normal form. The normal form is now codimension-two:

$$\mathcal{H} : A \mapsto A(-1 - \tilde{\varepsilon} - \tilde{\eta}|A|^2 + \tilde{a}|A|^4), \quad \tilde{a} \in \mathbb{R}, \ \ \tilde{a} \neq 0. \tag{37}$$

The only fixed point is the basic state, $A = 0$. Depending on the values of $\tilde{\varepsilon}$ and $\tilde{\eta}$, there are either 0, 1 or 2 invariant circles of period doubled bifurcated solutions. The corresponding regions in $(\tilde{\varepsilon}, \tilde{\eta})$-space where these exist are labeled (i), (ii) and (iii), respectively, in Fig. 10, where the case $\tilde{a} > 0$ is shown. If $\tilde{a} < 0$, Fig. 10 must be reflected through the vertical axis. The solid line $\tilde{\varepsilon} = 0$ is a line of period-doubling bifurcations. The curve separating regions

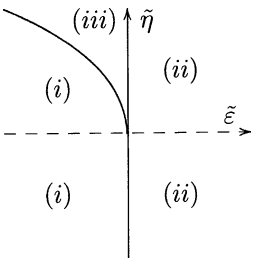

Fig. 10. Regions in parameter space with 0 (region (i)), 1 (region (ii)) and 2 (region (iii)) bifurcating circles of solutions.

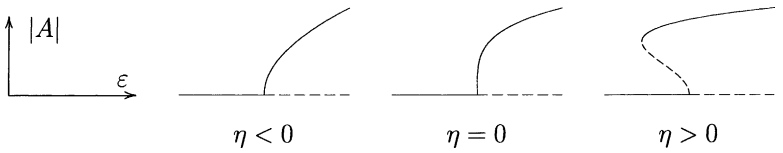

Fig. 11. Amplitude A of the bifurcated solutions as a function of ε. The circle of bifurcated solutions can be obtained by rotation around the horizontal axis. Solid (dashed) lines correspond to stable (unstable) states. The horizontal axis is the basic state.

(i) and (iii) is a line of saddle-node bifurcations of period-two solutions, and it is given by $\tilde{\eta} = 2(-a\tilde{\varepsilon})^{1/2}$. The symmetries of the bifurcated solutions are exactly the same as in the non-degenerate case.

The normal form for the Poincaré map in the degenerate case is given by

$$\mathcal{P} : A \mapsto A(1 + \varepsilon + \eta|A|^2 - a|A|^4), \quad \varepsilon = 2\tilde{\varepsilon}, \quad \eta = 2\tilde{\eta}, \quad a = 2\tilde{a}, \tag{38}$$

where higher order terms in A, ε and η have been neglected as before; the normal form is valid in a neighborhood of the origin where $\eta = \mathrm{O}(\varepsilon^{1/4})$ and $A = \mathrm{O}(\varepsilon^{1/2})$. All the bifurcated states are fixed points of $\mathcal{P}$, and the bifurcation is a degenerate pitchfork of revolution. In Fig. 11, the fixed points of $\mathcal{P}$ are plotted as functions of ε, showing that the pitchfork bifurcation is supercritical for $\eta < 0$, subcritical for $\eta > 0$, and $\eta = 0$ is the degenerate case.

Fig. 12 shows the nonlinear growth of the perturbation amplitude for the mode A instability of the periodically driven cavity flow at ($St = 160$, $Re = 1250$), where $\varepsilon = 0.0141$. The curve adjusts very well to the normal form expression for $\mathcal{P}$, (38), and the fitted coefficients are $\eta = 55V_{\max}^{-2} \approx 0$ and $a = 6.7 \times 10^5 V_{\max}^{-4}$.

Fig. 13 shows the growth of q_z as a function of Re. Instead of the linear growth corresponding to the non-degenerate case, we have a square root behavior, that corresponds to $\eta \approx 0$; from (38), $q_z \propto |A|^2 \propto \varepsilon^{1/2} \propto |Re - Re_c|^{1/2}$.

5.3. Normal form for $\mathcal{F}_4^c$: non-resonant Neimark–Sacker bifurcation

As before, the normal form is first computed for $\mathcal{H}$ and then for $\mathcal{P}$. In this case, there are a pair of complex-conjugate Floquet multipliers, $\mu_H = \mathrm{e}^{\pm \mathrm{i}\theta/2}, \theta \in (0, 2\pi)$, that have multiplicity 2. The center manifold $\mathcal{M}_c$ is four-dimensional, and the actions of L_H and O(2) are given by the joint representation $\mathcal{F}_4^c$, (23), in a basis $\{\boldsymbol{U}, \boldsymbol{V}, \bar{\boldsymbol{U}}, \bar{\boldsymbol{V}}\}$. The actions of L_H, R_α and K_z on the amplitudes A and B of $\boldsymbol{U}$ and $\boldsymbol{V}$ are given by

$$L_H = \begin{pmatrix} \mathrm{e}^{\mathrm{i}\theta/2} & 0 \\ 0 & \mathrm{e}^{\mathrm{i}\theta/2} \end{pmatrix}, \qquad R_\alpha = \begin{pmatrix} \mathrm{e}^{\mathrm{i}\beta\alpha} & 0 \\ 0 & \mathrm{e}^{-\mathrm{i}\beta\alpha} \end{pmatrix}, \qquad K_z = \begin{pmatrix} 0 & 1 \\ 1 & 0 \end{pmatrix} \tag{39}$$

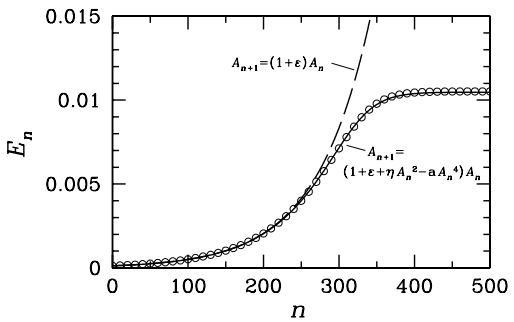

Fig. 12. Nonlinear growth of a measure of perturbation amplitude for the mode A instability of the periodically driven cavity at ($St = 160$, $Re = 1250$). In order to avoid clutter, only every tenth cycle is represented.

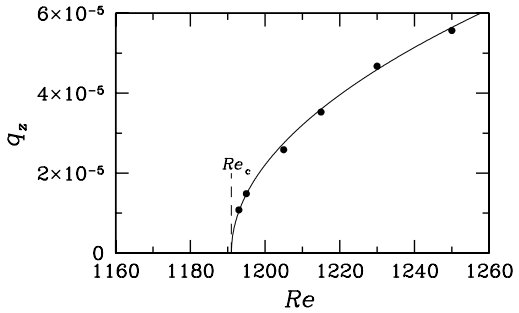

Fig. 13. Analysis of the growth in energy of the saturated perturbation flow, q_z with departure from the critical Reynolds number $Re_c = 1191$ at $St = 160$ for mode A of the cavity flow.

and the actions on $\bar{A}$ and $\bar{B}$ are given by the corresponding complex-conjugate matrices. The normal form for $\mathcal{H}$ in the non-resonant case ($\theta/2\pi$ irrational) is (Appendix B.2):

$$A \mapsto A[e^{i\theta/2} + P(|A|^2, |B|^2, \varepsilon)], \qquad B \mapsto B[e^{i\theta/2} + P(|B|^2, |A|^2, \varepsilon)]. \tag{40}$$

Up to third order in A and B, the normal form is

$$\mathcal{H}: \begin{cases} A \mapsto A(e^{i\theta/2} + \hat{\varepsilon} + \hat{a}|A|^2 + \hat{b}|B|^2), \\ B \mapsto B(e^{i\theta/2} + \hat{\varepsilon} + \hat{a}|B|^2 + \hat{b}|A|^2), \end{cases} \qquad \hat{\varepsilon}, \hat{a}, \hat{b} \in \mathbb{C}. \tag{41}$$

Introducing the moduli and phases of $A = r_1 e^{i\phi_1}$ and $B = r_2 e^{i\phi_2}$, the normal form becomes

$$\mathcal{H}: \begin{cases} r_1 \mapsto r_1(1 + \tilde{\varepsilon} - \tilde{a}r_1^2 - \tilde{b}r_2^2), \\ r_2 \mapsto r_2(1 + \tilde{\varepsilon} - \tilde{a}r_2^2 - \tilde{b}r_1^2), \\ \phi_1 \mapsto \phi_1 + \dfrac{\theta}{2} + \eta + cr_1^2 + dr_2^2, \\ \phi_2 \mapsto \phi_2 + \dfrac{\theta}{2} + \eta + cr_2^2 + dr_1^2, \end{cases} \qquad \tilde{\varepsilon}, \eta, \tilde{a}, \tilde{b}, c, d \in \mathbb{R}. \tag{42}$$

This is a codimension-two bifurcation containing two real parameters $\tilde{\varepsilon}$ and η. Nevertheless, the dynamics of ϕ_1 and ϕ_2 are trivial; the phases increase approximately by $\theta/2$ every half-period $T/2$, and are slightly modulated by the coefficients c and d and the moduli $r_1 = |A|$ and $r_2 = |B|$. The dynamics of r_1 and r_2 are decoupled from the phase dynamics, and we effectively end up with a codimension-one two-dimensional map for r_1 and r_2:

$$\mathcal{H}: \begin{cases} r_1 \mapsto r_1(1 + \tilde{\varepsilon} - \tilde{a}r_1^2 - \tilde{b}r_2^2), \\ r_2 \mapsto r_2(1 + \tilde{\varepsilon} - \tilde{a}r_2^2 - \tilde{b}r_1^2), \end{cases} \qquad \tilde{\varepsilon}, \tilde{a}, \tilde{b} \in \mathbb{R}. \tag{43}$$

The normal form for the Poincaré map is

$$\mathcal{P}: \begin{cases} r_1 \mapsto r_1(1 + \varepsilon - ar_1^2 - br_2^2), \\ r_2 \mapsto r_2(1 + \varepsilon - ar_2^2 - br_1^2), \end{cases} \qquad \varepsilon = 2\tilde{\varepsilon}, \quad a = 2\tilde{a}, \quad b = 2\tilde{b}. \tag{44}$$

The phase dynamics for $\mathcal{P}$ are the same as for $\mathcal{H}$, with the phases ϕ_1 and ϕ_2 increasing by θ every period T of $\mathcal{P}$. In the (non-resonant) quasi-periodic case, there are no differences between the normal forms for $\mathcal{H}$ and $\mathcal{P}$. The result is analogous to that for the Hopf bifurcation with O(2) symmetry, and the subsequent analysis follows closely that of [10]. We present the results for $\mathcal{P}$; substituting $\varepsilon = 2\tilde{\varepsilon}$, $a = 2\tilde{a}$ and $b = 2\tilde{b}$ gives the corresponding results for $\mathcal{H}$.

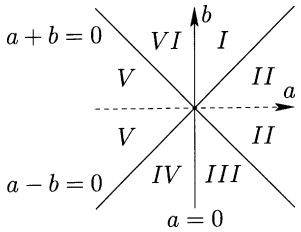

Fig. 14. Regions in (a, b)-parameter space for the normal form (44), where different phase portraits exist. The corresponding phase portraits are shown in Fig. 15.

The normal form (44) has four different fixed points:

$$p_0 = (0, 0), \tag{45}$$

$$p_1 = \left(\left[\frac{\varepsilon}{a}\right]^{1/2}, 0\right), \tag{46}$$

$$p_2 = \left(0, \left[\frac{\varepsilon}{a}\right]^{1/2}\right), \tag{47}$$

$$p_3 = \left(\left[\frac{\varepsilon}{a+b}\right]^{1/2}, \left[\frac{\varepsilon}{a+b}\right]^{1/2}\right). \tag{48}$$

p_0 exists for all values of ε, and is stable iff $\varepsilon < 0$; p_1 and p_2 exist only for $\varepsilon/a > 0$, and are stable iff $\varepsilon > 0$ and $(a-b)/a < 0$; and p_3 exists only for $\varepsilon/(a+b) > 0$, and it is stable iff $\varepsilon > 0$ and $(a-b)/(a+b) > 0$ (Appendix B.2).

In (a, b)-parameter space, there are six different regions separated by three bifurcation curves: $a = 0$, where p_1 and p_2 disappear going to infinity; $a + b = 0$, where p_3 disappears going to infinity; and $a - b = 0$, where one of the eigenvalues of p_1, p_2 and p_3 changes sign. These six regions are drawn in Fig. 14, and phase portraits for $\varepsilon < 0$ and $\varepsilon > 0$ are drawn for the six regions in Fig. 15. In these phase portraits, when ε crosses zero, p_1, p_2 and p_3 simultaneously collide with p_0 and are born or destroyed.

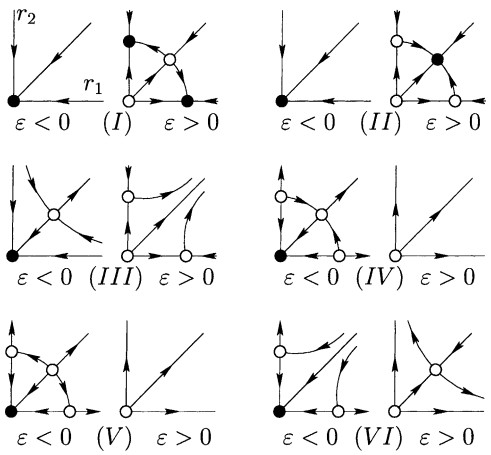

Fig. 15. Phase portraits corresponding to the six regions in Fig. 14. p_0 is the fixed point at the origin, p_1 lies on the horizontal (r_1) axis, p_2 lies on the vertical (r_2) axis, and p_3 is on the bisector. Solid (hollow) points are stable (unstable).

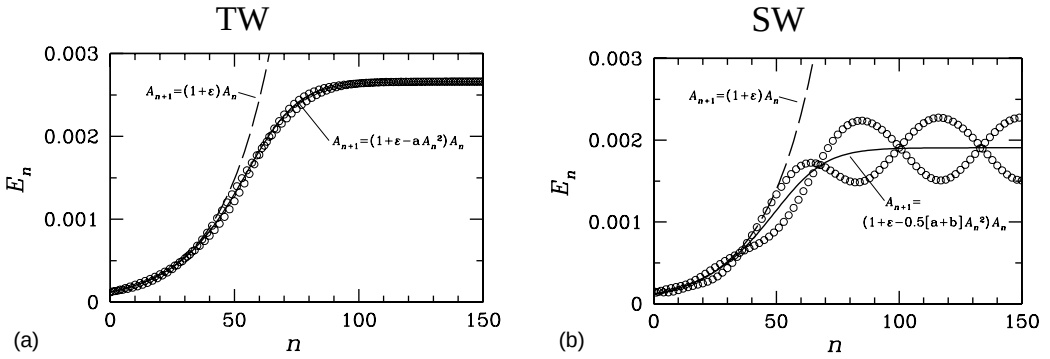

Fig. 16. Nonlinear growth of a measure of perturbation amplitude for the mode QP instability of the periodically driven cavity at $St = 100$ and $Re = 1225$. Every cycle is represented.

The equilibria p_1, p_2 and p_3 are represented as fixed points in Fig. 15, where only r_1 and r_2 coordinates are displayed. However, the center manifold is four-dimensional, and we must also consider the two phases ϕ_1 and ϕ_2; these phases correspond to independent rotations in the planes $(A, \bar{A})$ and $(B, \bar{B})$. In doing so, p_1 and p_2 become circles ($\mathbb{T}^1$), and p_3 becomes a two torus ($\mathbb{T}^2$). These $\mathbb{T}^1$ and $\mathbb{T}^2$ are located in the Poincaré section of the original dynamical system. Considered as invariant manifolds (by time evolution) of the original system, p_1 and p_2 are two-tori ($\mathbb{T}^2$) and p_3 is a three-torus ($\mathbb{T}^3$). As we shall see, however, p_3 is a $\mathbb{T}^2$ because both phases ϕ_1 and ϕ_2 have exactly the same frequency; what we have is a continuous family of invariant (by time evolution) $\mathbb{T}^2$ that together span a $\mathbb{T}^3$.

Fig. 16 shows the nonlinear growth of E_n for the mode QP instability of the periodically driven cavity flow at $St = 100$ and $Re = 1225$, where $\varepsilon = 0.0513$. For modulated traveling waves (TW), Fig. 16(a), E_n fits very well to the normal form expression for p_1 and p_2, while for modulated standing waves (SW), Fig. 16(b), E_n exhibits oscillations absent in the normal form expression for p_3. Introducing $A_n = (r_1^2 + r_2^2)^{1/2}$ as a measure of the amplitude, we obtain from (44):

$$\text{TW}: \quad A_{n+1} = A_n(1 + \varepsilon - aA_n^2), \tag{49}$$

$$\text{SW}: \quad A_{n+1} = A_n(1 + \varepsilon - 0.5[a + b]A_n^2). \tag{50}$$

The velocity field of the TW solutions after a period is the same as the initial field, except for a translation in z (see Fig. 17). Therefore E_n, which is an integrated quantity over a spanwise wavelength, does not contain the second frequency of the TW solution, that manifests only as a spanwise translation. E_n then follows (49). This is clearly seen in Fig. 16(a); the small oscillation present is a transient that decays for large n. At $St = 100$ and $Re = 1225$, the saturation value E_∞ provides $a = 7.25 \times 10^3 V_{\max}^{-2}$.

For the SW solutions the situation is more complicated. The second frequency is not associated with any symmetry operation, and it is not easy to find a measure of the amplitude of the solution. Fig. 16(b) shows that E_n is not proportional to the amplitude (in the normal form sense) of the SW, but contains oscillations with the second frequency of the flow. The detailed form of the oscillatory behavior is a combined consequence of the real projection of the perturbation mode amplitude oscillating harmonically at the secondary frequency [4], and E_n containing contributions from all locations in the domain, where the perturbation amplitudes are not required to have the same temporal phase. The solid line in Fig. 16(b) shows that averaging over the second frequency oscillations, the curve obtained (solid line) fits very well the normal form prediction (50). At $St = 100$ and $Re = 1225$, the saturation value E_n provides $0.5(a + b) = 14.1 \times 10^3 V_{\max}^{-2}$. Using the value of a obtained from the TW solutions, we obtain

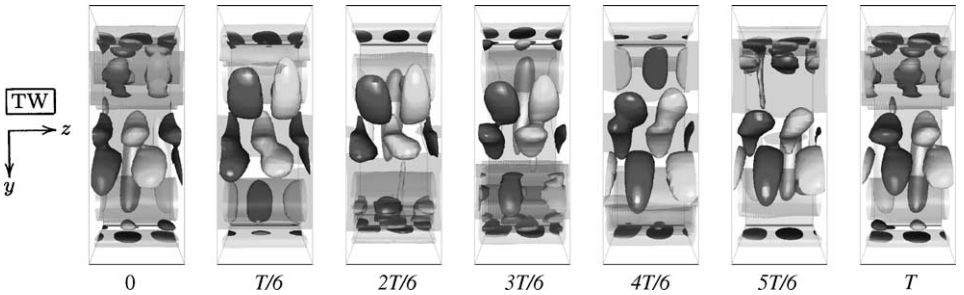

Fig. 17. Vorticity dynamics of modulated $+z$-traveling waves for the joint representation $\mathcal{F}_4^c$ in the periodically driven cavity flow [4], shown in a spanwise (z) domain extent of one wavelength, at $St = 100$ and $Re = 1225$. Solid isosurfaces are of the out-of-page (x) component of vorticity, positive and negative of equal magnitude, while translucent isosurfaces represent the z-component of vorticity. The driven cavity wall lies further into the page than the structures, and oscillates in the $\pm y$-direction.

$b = 20.95 \times 10^3 V_{\max}^{-2} > 7.25 \times 10^3 V_{\max}^{-2} = a$, in full agreement with the normal form theory prediction $b > a$. This corresponds to Case I, Fig. 15, where TW solutions are stable.

Consider the action of O(2), $\mathcal{H}$ and $\mathcal{P}$ (Eqs. (39), (42) and (44), respectively) on the solutions p_1 and p_2. As the moduli r_1 and r_2 do not change, let us focus on the respective phases ϕ_1 (for p_1) and ϕ_2 (for p_2). From (39) we obtain

$$p_1: \quad \mathcal{H}\phi_1 = \phi_1 + \tfrac{1}{2}\tilde{\theta}, \qquad \mathcal{P}\phi_1 = \phi_1 + \tilde{\theta}, \qquad R_\alpha \phi_1 = \phi_1 + \beta\alpha, \tag{51}$$

$$p_2: \quad \mathcal{H}\phi_2 = \phi_2 + \tfrac{1}{2}\tilde{\theta}, \qquad \mathcal{P}\phi_2 = \phi_2 + \tilde{\theta}, \qquad R_\alpha \phi_2 = \phi_2 - \beta\alpha, \tag{52}$$

where $\tilde{\theta} = \theta + 2\eta + 2c\varepsilon/a$ (from (42) and (46)). p_1 and p_2 are K_z-conjugate, K_z transforms one into the other. The action of $\mathcal{H}$ and $\mathcal{P}$ (advancing in time) is exactly the same as the action of an appropriate SO(2) element (a specific translation R_α in the spanwise z-direction). Therefore p_1 and p_2 are traveling waves in z, and they travel in opposite directions. As the action of $\mathcal{P}$ coincides with the action of $R_{\tilde{\theta}/\beta}$, the phase velocity is $c_z = \pm\tilde{\theta}/T\beta$, where T is the forcing period; the plus sign corresponds to p_1 and the minus sign to p_2. Notice that the phase velocity at criticality is given by the imaginary part of the critical eigenvalue, $c_z = \theta/T\beta$, and varies linearly with the parameters in a neighborhood of the bifurcation point: $c_z = (\theta + 2\eta + 2c\varepsilon/a)/T\beta$; this linear dependence can be used to estimate the normal form constant c/a. Although we use the term *traveling wave* for these solutions, p_1 and p_2, they are *not* true traveling waves: due to the time-dependent nature of the basic state, we do not have a fixed pattern translating in space as time evolves, but rather we have a time-dependent pattern that after a forcing period T has exactly the same form as that at the beginning of the period, but translated in space; a *modulated traveling wave* (TW). A given solution is not invariant by the action of R_α, but becomes a different solution on the $\mathbb{T}^2$; it is the $\mathbb{T}^2$ that is R_α [and SO(2)] invariant.

The modulated traveling waves p_1 and p_2 break the K_z symmetry. p_1 and p_2 live on two invariant $\mathbb{T}^2$, by time evolution and by SO(2); K_z transforms one $\mathbb{T}^2$ into the other. For these traveling waves, advancing time by the period T is the same as a z-translation; and the action of the spatio-temporal symmetry $\mathcal{H}$ is also the same as a z-translation. Although $\mathcal{H}$ symmetry is not preserved (it changes the phase ϕ), there is still a preserved spatio-temporal symmetry, the combination $\mathcal{H}R_{-\tilde{\theta}/2\beta}$, i.e. in a frame of reference translating in z at the phase speed, p_1 and p_2 appear $\mathcal{H}$-invariant. All these symmetries of the TW have been observed in the numerically computed solutions for the driven cavity flow, and many of them are apparent from Fig. 17.

Isosurfaces of vorticity of modulated traveling waves (TW) of the periodically driven cavity flow computed at $St = 100$ and $Re = 1225$, which is at a Reynolds number just slightly above the bifurcation ($Re_c = 1212$ at $St = 100$) are shown in Fig. 17. We see from the figure that the second frequency introduced by the Neimark–Sacker

bifurcation manifests itself as a translation in z after advancing a forcing period in time. The action of $\mathcal{H}$ is also equivalent to a z-translation. The K_z symmetry is broken, and applying it changes the sign of the z-translation, so the resulting TW moves in the opposite direction.

Now consider the action of O(2), $\mathcal{H}$ and $\mathcal{P}$ on p_3. As the moduli r_1 and r_2 do not change, we focus on the phases ϕ_1 and ϕ_2. To simplify the discussion, let

$$\phi = \tfrac{1}{2}(\phi_1 + \phi_2), \qquad \psi = \tfrac{1}{2}(\phi_1 - \phi_2). \tag{53}$$

From (39) we obtain

$$\mathcal{H}\begin{pmatrix}\phi\\ \psi\end{pmatrix} = \begin{pmatrix}\phi + \frac{1}{2}\hat{\theta}\\ \psi\end{pmatrix}, \qquad \mathcal{P}\begin{pmatrix}\phi\\ \psi\end{pmatrix} = \begin{pmatrix}\phi + \hat{\theta}\\ \psi\end{pmatrix}, \tag{54}$$

$$R_\alpha\begin{pmatrix}\phi\\ \psi\end{pmatrix} = \begin{pmatrix}\phi\\ \psi + \beta\alpha\end{pmatrix}, \qquad K_z\begin{pmatrix}\phi\\ \psi\end{pmatrix} = \begin{pmatrix}\phi\\ -\psi\end{pmatrix}, \tag{55}$$

where $\hat{\theta} = \theta + 2\eta + 2(c+d)\varepsilon/(a+b)$. Both $\mathcal{H}$ and $\mathcal{P}$ leave ψ invariant (54), and so time evolution (iterates of $\mathcal{P}$ and $\mathcal{H}$) only modifies the phase ϕ. The $\mathbb{T}^2$ obtained by keeping $\psi = \psi_0$ constant contains any solution obtained with the given ψ_0 as initial condition. Any p_3 solution lies on a $\mathbb{T}^2$, and as it is a linear combination of two equal amplitude modulated traveling waves, traveling in opposite directions, we call it a *modulated standing wave* (SW) solution. The O(2) symmetries R_α and K_z change ψ (55), and therefore the aforementioned $\mathbb{T}^2$ (with $\psi = \psi_0$) is not O(2)-invariant. Nevertheless, there is a particular combination of R_α and K_z that keeps ψ_0 invariant:

$$R_{\psi_0/\beta} K_z R_{-\psi_0/\beta}\begin{pmatrix}\phi\\ \psi_0\end{pmatrix} = \begin{pmatrix}\phi\\ \psi_0\end{pmatrix}. \tag{56}$$

This is a z-reflection, centered not about the origin $z = 0$, but about $z = \psi_0/\beta$. This is exactly the same behavior we found with the synchronous modes A and B corresponding to cases $\mathcal{F}_2^{\pm}$, and we say that K_z symmetry is preserved. SO(2) symmetry (translations in the spanwise direction) and $\mathcal{H}$ symmetry are broken (they change the phase ϕ), and SW do not retain any spatio-temporal symmetry, because all the space symmetries keep ϕ fixed.

All these symmetries of SW have been observed in the numerically computed solutions for the driven cavity flow, and many of them are apparent from Fig. 18, which shows vorticity isosurfaces at $St = 100$ and $Re = 1225$, which is at a Reynolds number just slightly above the bifurcation ($Re_c = 1212$ at $St = 100$). The figure shows that K_z is preserved, but the SW solution is fully quasi-periodic, in the sense that advancing in time is not equivalent to any

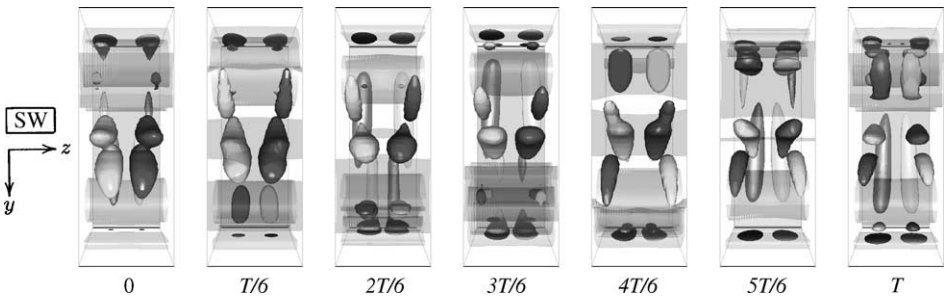

Fig. 18. Vorticity dynamics of modulated standing and traveling waves for the joint representation $\mathcal{F}_4^c$ in the periodically driven cavity flow [4], shown in a spanwise (z) domain extent of one wavelength, at $St = 100$ and $Re = 1225$. Solid isosurfaces are of the out-of-page (x) component of vorticity, positive and negative of equal magnitude, while translucent isosurfaces represent the z-component of vorticity. The driven cavity wall lies further into the page than the structures, and oscillates in the $\pm y$-direction.

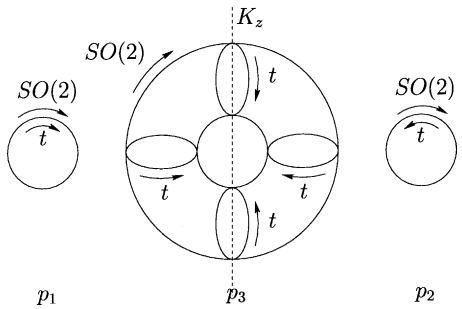

Fig. 19. Schematic of the standing and traveling wave solutions and their symmetries, on a Poincaré section. p_1 and p_2 are the two traveling waves, K_z-related. MSW solutions form the central $\mathbb{T}^2$, which is K_z-invariant; individual modulated standing wave solutions p_3 are not SO(2)-invariant, but are invariant under a conveniently translated (rotated in the plot) K_z symmetry. Time evolution is indicated by an arrow labeled t, and the action of SO(2) is also indicated.

space symmetry. Any non-trivial z-translation (not a multiple of the z-wavelength), produces a new solution of SW type.

In summary, modulated traveling wave solutions break Z_2 and retain SO(2), and so there exist two different modulated traveling waves, p_1 and p_2, that are Z_2-conjugates. Modulated standing wave solutions break SO(2) and retain Z_2, and so there exists a continuous family of $\mathbb{T}^2$ that span a $\mathbb{T}^3$. From one of the standing wave solutions (a $\mathbb{T}^2$), the action of SO(2) generates the $\mathbb{T}^3$, and this $\mathbb{T}^3$ is a manifold invariant by O(2) and by time evolution. The traveling wave solutions retain a spatio-temporal symmetry (different from $\mathcal{H}$), and the standing waves do not have any spatio-temporal symmetry at all. Fig. 19 shows a schematic of the standing and traveling wave solutions and their symmetries; the plots are in a Poincaré section, so the $\mathbb{T}^2$ and $\mathbb{T}^3$ are represented as $\mathbb{T}^1$ and $\mathbb{T}^2$, respectively. The dotted line is the flip line of the K_z symmetry; the elements of SO(2) are rotations into the plot plane.

The persistence of the p_1, p_2 and p_3 solutions under arbitrary small perturbations can be proved exactly with the same methods as those presented in [10]. Therefore, p_1, p_2, and p_3 are structurally stable (they persist under arbitrary but small perturbations). However, the phase dynamics on these $\mathbb{T}^2$ solutions depends on $\tilde{\theta} = \theta + 2\eta +$ constant being rational or irrational. In the rational case, we have periodic solutions on the $\mathbb{T}^2$, while in the irrational case we have quasi-periodic solutions densely filling the $\mathbb{T}^2$. Any small perturbation can transform one type of solution into the other, and the dynamics on the $\mathbb{T}^2$ is not structurally stable. We need a second parameter, η, to unfold the subtleties of the phase dynamics on the $\mathbb{T}^2$; these subtleties include the presence of Arnold tongues and frequency locking phenomena [12]. The bifurcation is truly of codimension-two, but the existence and stability properties of p_1, p_2, and p_3 are codimension-one properties. This is exactly the same situation as with the Neimark–Sacker bifurcation without symmetries [12].

In many problems, e.g. in fluid dynamics, the basic state p_0 is the only fixed point that exists for $\varepsilon < 0$, and p_1, p_2, and p_3 only exist for $\varepsilon > 0$. In this case, we have only two possible scenarios, the ones in regions I and II of Fig. 14. In region I, p_1 and p_2 are stable and p_3 is unstable; in region II we have the opposite situation: only p_3 is stable, whereas p_1 and p_2 are unstable. Which one of these scenarios takes place depends on the particular problem at hand. In region I (stable traveling waves) we have $a < b$; in region II, where the standing waves are stable, we have $a > b$. These conditions on the growth rate of the L_2-norm of the bifurcated perturbations of the basic state, lead to a *rule of thumb* that the stable solution corresponds to the one with the largest growth rate. From (46)–(48) we have

$$\|p_1\| = \|p_2\| = \left(\frac{\varepsilon}{a}\right)^{1/2}, \qquad \|p_3\| = \left[\frac{2\varepsilon}{a+b}\right]^{1/2} \tag{57}$$

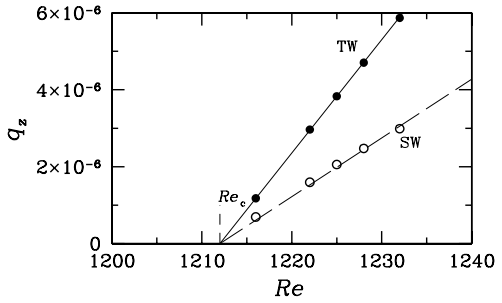

Fig. 20. The growth with Re for a measure of the perturbation energy for the saturated TW and SW states at $St = 100$ and $Re_c = 1212$. Solutions on the TW branch have largest energy, and are stable to perturbations; those on the SW branch have lower energy, and are unstable.

and $\|p_1\| > \|p_3\|$ iff $a < b$. In the driven cavity flow, the Neimark–Sacker bifurcation leads to scenario I dynamics, with TW being stable and $\|\mathrm{TW}\| > \|\mathrm{SW}\|$ [4,5]. This is also the case for the wake flows [3].

Fig. 20 shows the variation of q_z for TW and SW, for $St = 100$, as a function of Re. The growth rate of q_z with $|Re - Re_c|$ for TW is greater than that of SW—recall that the saturation coefficient for TW in Fig. 16 was greater than for SW—and the SW are unstable, according to the normal form analysis. We have been able to compute the unstable SW by time evolution (as shown in Fig. 18) by restricting the simulations to a K_z-invariant subspace where SW exist.

5.4. Normal form for $\mathcal{F}_4^c$: resonant cases and period doubling

The normal form for $\mathcal{H}$ in the resonant case ($\theta/2\pi$ rational) is (Appendix B.2):

$$\begin{aligned} A &\mapsto A[\mathrm{e}^{\mathrm{i}\pi k_1/k_2} + P(|A|^2, |B|^2, (AB)^{k_2}, (\overline{AB})^{k_2})] + \bar{A}^{k_2-1}\bar{B}^{k_2} Q(|A|^2, |B|^2, (AB)^{k_2}, (\overline{AB})^{k_2}),\\ B &\mapsto B[\mathrm{e}^{\mathrm{i}\pi k_1/k_2} + P(|B|^2, |A|^2, (AB)^{k_2}, (\overline{AB})^{k_2})] + \bar{A}^{k_2}\bar{B}^{k_2-1} Q(|B|^2, |A|^2, (AB)^{k_2}, (\overline{AB})^{k_2}), \end{aligned} \tag{58}$$

where P, Q are complex. The resonances do not modify the normal forms (43) and (44) up to fourth order, except in the special case $k_1/k_2 = 1/2$ where $\theta = \pi$, i.e. $\mu_H = \mathrm{e}^{\mathrm{i}\pi/2} = \mathrm{i}$ and $\mu_P = -1$. This is precisely the period-doubling case mentioned at the end of Section 4. As $\arg(\mu_H/2\pi) = 1/4$, this case corresponds to a 1:4 resonance for $\mathcal{H}$. In this case ($k_1/k_2 = 1/2$), the normal form up to third order is

$$\mathcal{H}: \begin{cases} A \mapsto A(\mathrm{i} + \hat{\varepsilon} + \hat{a}|A|^2 + \hat{b}|B|^2) + \hat{c}\bar{A}\bar{B}^2,\\ B \mapsto B(\mathrm{i} + \hat{\varepsilon} + \hat{a}|B|^2 + \hat{b}|A|^2) + \hat{c}\bar{A}^2\bar{B}, \end{cases} \tag{59}$$

where $\hat{\varepsilon}$, $\hat{a}$, $\hat{b}$ and $\hat{c} \in \mathbb{C}$; and for the Poincaré map $\mathcal{P}$:

$$\mathcal{P}: \begin{cases} A \mapsto A(-1 + \varepsilon + a|A|^2 + b|B|^2) + c\bar{A}\bar{B}^2,\\ B \mapsto B(-1 + \varepsilon + a|B|^2 + b|A|^2) + c\bar{A}^2\bar{B}, \end{cases} \tag{60}$$

where $\varepsilon = 2\mathrm{i}\hat{\varepsilon}$, $a = 2\mathrm{i}\hat{a}$, $b = 2\mathrm{i}\hat{b}$ and $c = 2\mathrm{i}\hat{c}$.

The analysis of these normal forms remains incomplete. Since the phase dynamics is now coupled with the amplitude dynamics through the resonant term, this is a codimension-two bifurcation which is not reducible to a codimension-one bifurcation as was possible in the non-resonant case. Period doubling in either the driven cavity flow or the wake flows has not yet been observed as a bifurcation directly from the basic state [3].

5.5. Normal form for $\mathcal{F}_4^s$: resonances 1:1 and 1:2

In this case, the center manifold $\mathcal{M}_c$ is also four-dimensional. The normal form for $\mathcal{H}$ in the amplitudes A, B, $\bar{A}$ and $\bar{B}$, corresponding to $\mathcal{F}_4^s$ (24), is of the form (Appendix B.3):

$$\begin{aligned} &A \mapsto A[s + P(|A|^2, \bar{A}B - A\bar{B}, \varepsilon)], \\ &B \mapsto B[s + P(|A|^2, \bar{A}B - A\bar{B}, \varepsilon)] + A[\delta_H + Q(|A|^2, \bar{A}B - A\bar{B}, \eta)], \end{aligned} \tag{61}$$

plus the complex-conjugate equations giving the action of the map on $\bar{A}$ and $\bar{B}$. The normal form for $\mathcal{H}$ up to third order is

$$\mathcal{H}: \begin{cases} A \mapsto A(s + \hat{\varepsilon} + \hat{a}|A|^2 + \hat{b}(\bar{A}B - A\bar{B})), \\ B \mapsto B(s + \hat{\varepsilon} + \hat{a}|A|^2 + \hat{b}(\bar{A}B - A\bar{B})) + A(\delta_H + \hat{\eta} + \hat{c}|A|^2 + \hat{d}(\bar{A}B - A\bar{B})), \end{cases} \tag{62}$$

where $\hat{\varepsilon}$, $\hat{\eta}$, $\hat{a}$, $\hat{b}$, $\hat{c}$ and $\hat{d}$ are real. These are codimension-two bifurcations, with bifurcation parameters $\hat{\varepsilon}$, $\hat{\eta}$, and with four coefficients ($\hat{a}$, $\hat{b}$, $\hat{c}$ and $\hat{d}$), reminiscent of the strong 1:1 ($s = 1$) and 1:2 ($s = -1$) resonances (e.g. see [12]), but more involved because here the amplitudes A and B are complex. The normal form for the Poincaré map $\mathcal{P}$ is

$$\mathcal{P}: \begin{cases} A \mapsto A[1 + \varepsilon + a|A|^2 + b(\bar{A}B - A\bar{B})], \\ B \mapsto B[1 + \varepsilon + a|A|^2 + b(\bar{A}B - A\bar{B})] + A\delta_P + \eta + c|A|^2 + d(\bar{A}B - A\bar{B})], \end{cases} \tag{63}$$

where $\varepsilon = 2s\hat{\varepsilon}$, $\delta_P = 2s\delta_H$, $\eta = 2(s\hat{\eta} + \delta_H\hat{\varepsilon})$, $a = 2s\hat{a}$, $b = 2s\hat{b}$, $c = 2(s\hat{c} + \delta_H\hat{a})$ and $d = 2(s\hat{d} + \delta_H\hat{b})$; usually $\delta_P = 1$. As we have already found in the analysis of $\mathcal{F}_2^s$, the normal form for the Poincaré map $\mathcal{P}$ does not distinguish between the cases $s = \pm 1$, but they are clearly different for $\mathcal{H}$. The analysis of these normal forms remains to be done.

5.6. Normal form for $\mathcal{F}_2^{s_1} \oplus \mathcal{F}_2^{s_2}$: non-resonant case

In a convenient basis $\{\boldsymbol{U}, \bar{\boldsymbol{U}}\}$ of $\mathcal{F}_2^{s_1}$ and $\{\boldsymbol{V}, \bar{\boldsymbol{V}}\}$ of $\mathcal{F}_2^{s_2}$, the action of O(2) and L_H in the corresponding amplitudes A, $\bar{A}$, B and $\bar{B}$, is

$$R_\alpha = \begin{pmatrix} e^{i\beta_1\alpha} & 0 & 0 & 0 \\ 0 & e^{-i\beta_1\alpha} & 0 & 0 \\ 0 & 0 & e^{i\beta_2\alpha} & 0 \\ 0 & 0 & 0 & e^{-i\beta_2\alpha} \end{pmatrix}, \qquad K_z = \begin{pmatrix} 0 & 1 & 0 & 0 \\ 1 & 0 & 0 & 0 \\ 0 & 0 & 0 & 1 \\ 0 & 0 & 1 & 0 \end{pmatrix}, \qquad L_H = \begin{pmatrix} s_1 & 0 & 0 & 0 \\ 0 & s_1 & 0 & 0 \\ 0 & 0 & s_2 & 0 \\ 0 & 0 & 0 & s_2 \end{pmatrix}. \tag{64}$$

We assume different β-values in each $\mathcal{F}_2^s$. The normal form for $\mathcal{H}$ in the non-resonant case (β_1/β_2 irrational) can be written as (Appendix B.3):

$$A \mapsto A[s_1 + P(|A|^2, |B|^2, \varepsilon)], \qquad B \mapsto B[s_2 + Q(|A|^2|, B|^2, \eta)] \tag{65}$$

and the normal forms for $\mathcal{H}$ and $\mathcal{P}$ up to third order are

$$\mathcal{H}: \begin{cases} A \mapsto A(s_1 + \hat{\varepsilon} + \hat{a}|A|^2 + \hat{b}|B|^2), \\ B \mapsto B(s_2 + \hat{\eta} + \hat{c}|A|^2 + \hat{d}|B|^2), \end{cases} \tag{66}$$

$$\mathcal{P}: \begin{cases} A \mapsto A(1+\varepsilon+a|A|^2+b|B|^2), \\ B \mapsto B(1+\eta+c|A|^2+d|B|^2), \end{cases} \tag{67}$$

where all the coefficients and parameters are real, and $\varepsilon = 2s_1\hat{\varepsilon}$, $a = 2s_1\hat{a}$, $b = 2s_1\hat{b}$, $\eta = 2s_2\hat{\eta}$, $c = 2s_2\hat{c}$ and $d = 2s_2\hat{d}$. Again, the normal forms for $\mathcal{H}$ distinguish between the different values of s_1 and s_2, but the normal forms for $\mathcal{P}$ do not. These normal forms are of codimension-two, and the normal form for $\mathcal{P}$ has been analyzed (including one of the fifth order terms) in [2], where they describe possible interactions between the synchronous modes A and B (corresponding to $\mathcal{F}_2^-$ and $\mathcal{F}_2^+$, respectively) in the wake of a circular cylinder in terms of a mixed mode, $\mathcal{F}_2^+ \oplus \mathcal{F}_2^-$.

5.7. Normal form for $\mathcal{F}_2^{s_1} \oplus \mathcal{F}_2^{s_2}$: resonant case

The normal form for $\mathcal{H}$ in the resonant case ($\beta_1/\beta_2 = r/s$ rational) can be written as (Appendix B.3):

$$\begin{aligned} A &\mapsto A[s_1 + P_1(|A|^2, |B|^2, \bar{A}^s B^r, A^s \bar{B}^r, \varepsilon)] + \bar{A}^{s-1} B^r P_2(|A|^2, |B|^2, \bar{A}^s B^r, A^s \bar{B}^r, \eta), \\ B &\mapsto B[s_2 + Q_1(|A|^2, |B|^2, \bar{A}^s B^r, A^s \bar{B}^r, \lambda)] + A^s \bar{B}^{r-1} Q_2(|A|^2, |B|^2, \bar{A}^s B^r, A^s \bar{B}^r, \rho), \end{aligned} \tag{68}$$

where the polynomials P and Q are real. If $r + s \geq 5$, the resonant terms appear at fourth order or higher, and up to third order the normal form is the same as in the non-resonant case. In any case, these bifurcations are of codimension-two or greater, and their analysis has not been done yet, except in the particular case mentioned at the end of the preceding section.

6. Conclusions

The transition from two-dimensional to three-dimensional flow implies a breaking of the translational component of the spatial O(2) symmetry and that the center manifold has even dimension. With two-dimensional center manifolds, there are only two types of possible bifurcations leading to three-dimensional states. While these are both synchronous, one preserves the spatio-temporal $\mathcal{H}$ symmetry ($\mathcal{F}_2^+$), whereas the other breaks $\mathcal{H}$ symmetry ($\mathcal{F}_2^-$). With four-dimensional center manifolds, there are a number of possibilities that generally lead to non-synchronous states, described by two families of joint representations, $\mathcal{F}_4^c$ and $\mathcal{F}_4^s$. The $\mathcal{F}_4^c$ cases, in the absence of resonances, correspond to Neimark–Sacker bifurcations in which the phase dynamics are trivial and they are essentially codimension-one bifurcations. The breaking of O(2) symmetry in the four-dimensional case spawns two classes of nonlinear states: traveling waves and standing waves, both types modulated by the time-periodic basic state.

The lowest dimension of the center manifold that can support period doubling is four, and these are a resonant case of the $\mathcal{F}_4^c$ Neimark–Sacker bifurcations, corresponding to the 1:4 resonance. The other resonances (except for 1:1 and 1:2) share the same normal form, up to fourth order, as the non-resonant Neimark–Sacker. The 1:4 resonance (period doubling) is a codimension-two bifurcation, whereas all the other Neimark–Sackers are essentially codimension-one bifurcations with trivial phase dynamics. The $\mathcal{F}_4^s$ cases correspond to the 1:1 and 1:2 resonance cases, with $s = +$ and $s = -$, respectively. They are codimension-two bifurcations, so only occur at a point in (Re, St)-space, and so one may expect to find them somewhere along the Neimark–Sacker curve (like other resonances); the difference is that these resonances have particular dynamics associated with them. Little is yet known in detail; see [12] for a discussion of the generic 1:1 and 1:2 resonances that occur without additional complications from symmetries, which make the normal form amplitudes complex. With a four-dimensional center manifold, there can also be three-dimensional mixed-mode solutions, corresponding to the various compositions between $\mathcal{F}_2^+$ and $\mathcal{F}_2^-$; these also are manifest via codimension-two bifurcations.

We have analyzed bifurcations where all the critical eigenfunctions break the spanwise translation symmetry SO(2), leading to three-dimensional flows. In terms of the decomposition $E_c = W_1 \oplus W_2$ mentioned at the beginning of Section 4, we have analyzed the case $W_1 = \{0\}$. The complementary case, $W_2 = \{0\}$, corresponds to bifurcations where the flow remains two-dimensional, i.e. z-independent. It is also possible to have bifurcations with both W_1 and W_2 non-trivial. These bifurcations lead to mixed modes with some eigenfunctions preserving SO(2) symmetry and other eigenfunctions breaking it. These mixed-mode bifurcations are of codimension-two or higher, and their analysis is left for future investigations.

Acknowledgements

This work was partially supported by MCYT grant BFM2001-2350 (Spain), NSF Grant CTS-9908599 (USA), the Australian Partnership for Advanced Computing's Merit Allocation Scheme, and the Australian Academy of Science's International Scientific Collaborations Program.

Appendix A. Four-dimensional joint representations of O(2) and L_H

In the four-dimensional case, the representation of O(2) in E_c is a direct sum of two irreducible representations of the form (18), and E_c is the direct sum of two two-dimensional subspaces: $E_c = V_1 \oplus V_2$. When the spanwise wavenumber of the two representations are different, $\beta_1 \neq \beta_2$, these two representations are not isomorphic, and any linear operator in E_c commuting with the representation leaves V_1 and V_2 invariant (see [9, Lemma 3.4]). Therefore, the joint representation of SO(2) and L_H also splits into a direct sum of two irreducible representations of the form $\mathcal{F}_2^s$, $s = \pm$.

When $\beta_1 = \beta_2 = \beta$, V_1 and V_2 are not necessarily L_H-invariant subspaces, and we need to find the general form of the operator L_H commuting with the representation of O(2). Let $\{\boldsymbol{U}, \bar{\boldsymbol{U}}\}$ and $\{\boldsymbol{V}, \bar{\boldsymbol{V}}\}$ be bases of V_1 and V_2, respectively, and let $A\boldsymbol{U} + \overline{A\boldsymbol{U}} + B\boldsymbol{V} + \overline{B\boldsymbol{V}}$ be an element of E_c. The action of O(2) and L_H on $(A, \bar{A}, B, \bar{B})$ is

$$R_\alpha = \begin{pmatrix} M_\alpha & 0 \\ 0 & M_\alpha \end{pmatrix}, \qquad K_z = \begin{pmatrix} N & 0 \\ 0 & N \end{pmatrix}, \qquad L_H = \begin{pmatrix} L_1 & L_2 \\ L_3 & L_4 \end{pmatrix}, \tag{A.1}$$

where we have used block notation, and the elements of the matrices are 2×2 complex matrices. In particular

$$M_\alpha = \begin{pmatrix} e^{i\beta\alpha} & 0 \\ 0 & e^{-i\beta\alpha} \end{pmatrix}, \qquad N = \begin{pmatrix} 0 & 1 \\ 1 & 0 \end{pmatrix}. \tag{A.2}$$

An easy computation using that L_H is a real operator that commutes with R_α and K_z, and that the representation (A.2) of O(2) is irreducible, shows that the four matrices L_i are real multiples of the 2×2-identity, $L_i = a_i \mathbf{1}_2$, $a_i \in \mathbb{R}$. Computing the eigenvalues of L_H gives

$$\det(L_H - \mu_H \mathbf{1}_4) = [(\mu_H - a_1)(\mu_H - a_4) - a_2 a_3]^2 = 0 \tag{A.3}$$

and the eigenvalues have multiplicity 2, $\mu_H^s = (a_1 + a_4 + s[(a_1 - a_4)^2 + 4\hat{a}_2\hat{a}_3]^{1/2})/2$, where $s = \pm 1$. As we are in the center manifold, the eigenvalues of the map L_H must have modulus one, and there are three cases to be considered.

Case I. $(\mathcal{F}_2^+ \oplus \mathcal{F}_2^-) : (a_1 - a_4)^2 + 4\hat{a}_2\hat{a}_3 > 0$.

The eigenvalues μ_H^s are real and different, therefore they must be $+1$ and -1, and $a_1 + a_4 = 0$, $a_1^2 + a_2 a_3 = 1$. The four eigenvectors are

$$\mu_H^+ = 1: \quad \begin{cases} e_1 = (a_1+1)\boldsymbol{U} + a_3 \boldsymbol{V}, \\ e_2 = (a_1+1)\bar{\boldsymbol{U}} + a_3 \bar{\boldsymbol{V}} = \bar{e}_1, \end{cases}$$

$$\mu_H^- = -1: \quad \begin{cases} e_3 = (a_1-1)\boldsymbol{U} + a_3 \boldsymbol{V}, \\ e_4 = (a_1-1)\bar{\boldsymbol{U}} + a_3 \bar{\boldsymbol{V}} = \bar{e}_3. \end{cases}$$

The actions of R_α, K_z and L_H on this base are

$$R_\alpha = \begin{pmatrix} M_\alpha & 0 \\ 0 & M_\alpha \end{pmatrix}, \qquad K_z = \begin{pmatrix} N & 0 \\ 0 & N \end{pmatrix}, \qquad L_H = \begin{pmatrix} \mathbf{1}_2 & 0 \\ 0 & -\mathbf{1}_2 \end{pmatrix}, \tag{A.4}$$

where we have used block notation. This is the compound representation $\mathcal{F}_2^+ \oplus \mathcal{F}_2^-$, with the same value of β in both components.

Case II. $(\mathcal{F}_4^c): (a_1 - a_4)^2 + 4a_2 a_3 < 0$.

The eigenvalues μ_H^+ and μ_H^- are complex conjugates, and $a_1 a_4 - a_2 a_3 = 1$. The four eigenvectors are

$$\mu_H^+ = \mathrm{e}^{\mathrm{i}\theta/2}: \quad \begin{cases} e_1 = a_2 \boldsymbol{U} + (\mathrm{e}^{\mathrm{i}\theta/2} - a_1)\boldsymbol{V}, \\ e_2 = a_2 \bar{\boldsymbol{U}} + (\mathrm{e}^{\mathrm{i}\theta/2} - a_1)\bar{\boldsymbol{V}}, \end{cases}$$

$$\mu_H^- = \mathrm{e}^{-\mathrm{i}\theta/2}: \quad \begin{cases} e_3 = a_2 \bar{\boldsymbol{U}} + (\mathrm{e}^{-\mathrm{i}\theta/2} - a_1)\bar{\boldsymbol{V}} = \bar{e}_1, \\ e_4 = a_2 \boldsymbol{U} + (\mathrm{e}^{-\mathrm{i}\theta/2} - a_1)\boldsymbol{V} = \bar{e}_2. \end{cases}$$

The actions of R_α, K_z and L_H on this base are

$$R_\alpha = \begin{pmatrix} M_\alpha & 0 \\ 0 & M_{-\alpha} \end{pmatrix}, \qquad K_z = \begin{pmatrix} N & 0 \\ 0 & N \end{pmatrix}, \qquad L_H = \begin{pmatrix} \mu_H \mathbf{1}_2 & 0 \\ 0 & \bar{\mu}_H \mathbf{1}_2 \end{pmatrix}, \tag{A.5}$$

where we have used block notation, and written $\mu_H = \mathrm{e}^{\mathrm{i}\theta/2}$. This is the representation $\mathcal{F}_4^c$.

Case III. $(\mathcal{F}_4^s): (a_1 - a_4)^2 + 4a_2 a_3 = 0$.

The four eigenvalues coincide, $\mu_H = s = (a_1 + a_4)/2$, and we have two possibilities, $s = \pm 1$. In this case, L_H does not diagonalize and the four generalized eigenvectors are

$$e_1 = a_2 \boldsymbol{U} + (s - a_1)\boldsymbol{V}, \qquad e_2 = \delta_H \boldsymbol{V}, \qquad e_3 = a_2 \bar{\boldsymbol{U}} + (s - a_1)\bar{\boldsymbol{V}} = \bar{e}_1, \qquad e_4 = \delta_H \bar{\boldsymbol{V}} = \bar{e}_2,$$

where δ_H is an arbitrary non-zero real number, usually taken as 1 or a value that simplifies L_P. The actions of R_α, K_z and L_H on this base are

$$R_\alpha = \begin{pmatrix} \mathrm{e}^{\mathrm{i}\beta\alpha}\mathbf{1}_2 & 0 \\ 0 & \mathrm{e}^{-\mathrm{i}\beta\alpha}\mathbf{1}_2 \end{pmatrix}, \qquad K_z = \begin{pmatrix} 0 & N \\ N & 0 \end{pmatrix}, \qquad L_H = \begin{pmatrix} N_\delta & 0 \\ 0 & N_\delta \end{pmatrix}, \tag{A.6}$$

where we have used block notation, and written

$$N_\delta = \begin{pmatrix} s & \delta_H \\ 0 & s \end{pmatrix}. \tag{A.7}$$

This is the representation $\mathcal{F}_4^c$.

The results obtained can be summarized as follows: the four-dimensional joint representations of O(2) and L_H are of the form $\mathcal{F}_4^c$, $\mathcal{F}_4^s$ and $\mathcal{F}_2^{s_1} \oplus \mathcal{F}_2^{s_2}$, and in the last case, the β-value of each of the $\mathcal{F}_2^s$-components can be different.

Appendix B. Normal forms

For some low-codimension bifurcations in finite-dimensional systems, dynamical systems theory provides a center manifold reduction and a normal form. For infinite-dimensional systems, certain technical requirements must be satisfied in order to invoke the theorem, see [15] for details; the Navier–Stokes equations for confined flows fulfill these requirements. The *normal form* is a low-dimensional, low-order polynomial system that captures the dynamics of the full nonlinear system in the neighborhood of the bifurcation (e.g. [10]). The normal form contains a number of parameters that unfold the bifurcation; the number of parameters being the codimension of the bifurcation considered. Arbitrary perturbations of the normal form are usually accounted for by these unfolding parameters (see [20] for details and examples), and they result in a topologically equivalent system preserving all the dynamics of the normal form; this is the case for the well-known local codimension-one bifurcations [12]. However, when the codimension of the system is 2 or greater, persistence of all the dynamical features of the normal form is not always guaranteed. One may still perform a normal form analysis on the original system, truncate at some finite (low) order and extract *some* of the characteristic dynamics of the original system. The derivation of the normal forms in the presence of symmetries in this appendix follows the method of [10].

B.1. Normal form for $\mathcal{F}_2^s$, $s = \pm 1$

The normal form for $\mathcal{H}$ is of the form:

$$A \mapsto sA + Q(A, \bar{A}, \varepsilon) \tag{B.1}$$

and to any given finite order in A and $\bar{A}$, the function Q satisfies (e.g. see [10]):

$$Q(L_H A, L_H \bar{A}) = L_H Q(A, \bar{A}), \tag{B.2}$$

$$Q(K_z A, K_z \bar{A}) = K_z Q(A, \bar{A}), \tag{B.3}$$

$$Q(R_\alpha A, R_\alpha \bar{A}) = R_\alpha Q(A, \bar{A}). \tag{B.4}$$

This results in $Q(A, \bar{A}, \varepsilon) = AP(|A|^2, \varepsilon)$, with P a real polynomial satisfying $P(|A|^2, 0) = \mathrm{O}(|A|^2)$.

Proof. The actions of K_z and R_α on A and $\bar{A}$ (and on Q and $\bar{Q}$) are

$$L_H A = sA, \qquad L_H \bar{A} = s\bar{A}, \tag{B.5}$$

$$K_z A = \bar{A}, \qquad K_z \bar{A} = A, \tag{B.6}$$

$$R_\alpha A = \mathrm{e}^{\mathrm{i}\beta\alpha} A, \qquad R_\alpha \bar{A} = \mathrm{e}^{-\mathrm{i}\beta\alpha} \bar{A}. \tag{B.7}$$

The action of L_H is the identity for $s = 1$, and coincides with $R_{\pi/\beta}$ for $s = -1$. Substituting the action of K_z and R_α into (B.3) and (B.4), we obtain

$$Q(\bar{A}, A) = \overline{Q(A, \bar{A})}, \qquad Q(\mathrm{e}^{\mathrm{i}\beta\alpha} A, \mathrm{e}^{-\mathrm{i}\beta\alpha} \bar{A}) = \mathrm{e}^{\mathrm{i}\beta\alpha} Q(A, \bar{A}),$$

valid for any value of α. Applying these relations to a monomial $cA^m \bar{A}^n$, $c \in \mathbb{C}$, we obtain $c \in \mathbb{R}$, $m = n + 1$, and Q contains only monomials of the form $cA|A|^{2n}$. □

B.2. Normal form for $\mathcal{F}_4^c$

The normal form for $\mathcal{H}$ is

$$A \mapsto \mathrm{e}^{\mathrm{i}\theta/2}A + \tilde{P}(A, B, \bar{A}, \bar{B}), \qquad B \mapsto \mathrm{e}^{\mathrm{i}\theta/2}B + \tilde{Q}(A, B, \bar{A}, \bar{B}) \tag{B.8}$$

and to any given finite order in A, B, $\bar{A}$ and $\bar{B}$, the functions $\tilde{P}$ and $\tilde{Q}$ satisfy

$$\tilde{P}(\mathrm{e}^{\mathrm{i}\theta/2}A, \mathrm{e}^{\mathrm{i}\theta/2}B, \mathrm{e}^{-\mathrm{i}\theta/2}\bar{A}, \mathrm{e}^{-\mathrm{i}\theta/2}\bar{B}) = \mathrm{e}^{\mathrm{i}\theta/2}\tilde{P}(A, B, \bar{A}, \bar{B}), \tag{B.9}$$

$$\tilde{P}(\mathrm{e}^{\mathrm{i}\beta\alpha}A, \mathrm{e}^{-\mathrm{i}\beta\alpha}B, \mathrm{e}^{-\mathrm{i}\beta\alpha}\bar{A}, \mathrm{e}^{\mathrm{i}\beta\alpha}\bar{B}) = \mathrm{e}^{\mathrm{i}\beta\alpha}\tilde{P}(A, B, \bar{A}, \bar{B}), \tag{B.10}$$

$$\tilde{Q}(A, B, \bar{A}, \bar{B}) = \tilde{P}(B, A, \bar{B}, \bar{A}) \tag{B.11}$$

for any value of α. $\tilde{Q}$ also satisfies (B.9) and (B.10), but these additional equations are obtained using (B.11), which in fact gives $\tilde{Q}$ once $\tilde{P}$ has been obtained, and so do not provide any additional information. Applying these relationships to a monomial $A^pB^q\bar{A}^m\bar{B}^n$, we obtain

$$p + q - m - n - 1 = k\frac{4\pi}{\theta}, \qquad p - q - m + n - 1 = 0, \tag{B.12}$$

where the integer k is not zero in the resonant case ($2\pi/\theta$ rational).

First consider the *non-resonant* case, where $\theta/2\pi$ is irrational and $k = 0$. Solving (B.12) for p and q we obtain $p = m + 1$ and $q = n$, and the monomials in $\tilde{P}$ must be of the form $A|A|^{2m}|B|^{2n}$. Therefore, $\tilde{P} = AP(|A|^2, |B|^2, \varepsilon)$ and $\tilde{Q} = BP(|B|^2, |A|^2, \varepsilon)$, i.e. we obtain (40).

In the *resonant* case $\theta/(2\pi) = k_1/k_2 \in (0, 1)$ is rational and (B.12) has additional solutions. We can take the fraction k_1/k_2 as irreducible with both k_1 and k_2 positive: $0 < k_1 < k_2$, and $k_2 \geq 2$. In (B.12), $p+q-m-n-1 = p+q-m-n-1+p-q-m+n-1 = 2(p-m-1)$ is even; and $4\pi k/\theta = 2kk_2/k_1$, so kk_2/k_1 is an integer, and since k_1/k_2 is irreducible, k must be a multiple of k_1 : $k = jk_1$. Finally, Eq. (B.12) can be written as

$$p - m - 1 = q - n = jk_2, \quad j \in \mathbb{Z}. \tag{B.13}$$

The monomials in $\tilde{P}$ are of the form $A^{jk_2+1}B^{jk_2}|A|^{2m}|B|^{2n}$, $j \in \mathbb{Z}$, i.e.

$$\tilde{P}(A, B, \bar{A}, \bar{B}) = AP(|A|^2, |B|^2, (AB)^{k_2}, (\overline{AB})^{k_2})] + \bar{A}^{k_2-1}\bar{B}^{k_2}Q(|A|^2, |B|^2, (AB)^{k_2}, (\overline{AB})^{k_2}). \tag{B.14}$$

The monomials in $\tilde{Q}$ are obtained from $\tilde{P}$ by interchanging A and B. This gives (58). For $j = 0$ we obtain the non-resonant case. The resonant monomial of lowest order in $\tilde{P}$ is $\bar{A}^{k_2-1}\bar{B}^{k_2}$, of order $2k_2 - 1$; since $k_2 \geq 2$, it is of order three for $k_1/k_2 = 1/2$, and of order greater than or equal to 5 in any other case.

Stability of the equilibria p_i (48), in the non-resonant case. The Jacobians of the system (44) at the four fixed points (48) are

$$J_0 = \begin{pmatrix} 1+\varepsilon & 0 \\ 0 & 1+\varepsilon \end{pmatrix}, \qquad J_3 = \begin{pmatrix} 1 - \dfrac{2a\varepsilon}{a+b} & -\dfrac{2b\varepsilon}{a+b} \\ -\dfrac{2b\varepsilon}{a+b} & 1 - \dfrac{2a\varepsilon}{a+b} \end{pmatrix}, \tag{B.15}$$

$$J_1 = \begin{pmatrix} 1-2\varepsilon & 0 \\ 0 & 1 + \dfrac{\varepsilon(a-b)}{a} \end{pmatrix}, \qquad J_2 = \begin{pmatrix} 1 + \dfrac{\varepsilon(a-b)}{a} & 0 \\ 0 & 1-2\varepsilon \end{pmatrix}. \tag{B.16}$$

Their eigenvalues are: for p_0, $1 + \varepsilon$ is double; p_1 and p_2 have eigenvalues $1 - 2\varepsilon$ and $1 + \varepsilon(b - a)/a$; and p_3 has $1 - 2\varepsilon$ and $1 + 2\varepsilon(b - a)/(a + b)$. A fixed point is stable iff their eigenvalues have moduli less than 1.

B.3. Normal form for $\mathcal{F}_4^s$

The normal form for $\mathcal{H}$ is

$$A \mapsto sA + \tilde{P}(A, B, \bar{A}, \bar{B}), \qquad B \mapsto \delta_H A + sB + Q(A, B, \bar{A}, \bar{B}), \tag{B.17}$$

plus the complex-conjugate equations. Due to the O(2) symmetry, the functions $\tilde{P}$ and $\tilde{Q}$ satisfy

$$\tilde{P}(\mathrm{e}^{\mathrm{i}\beta\alpha}A, \mathrm{e}^{\mathrm{i}\beta\alpha}B, \mathrm{e}^{-\mathrm{i}\beta\alpha}\bar{A}, \mathrm{e}^{-\mathrm{i}\beta\alpha}\bar{B}) = \mathrm{e}^{\mathrm{i}\beta\alpha}\tilde{P}(A, B, \bar{A}, \bar{B}), \tag{B.18}$$

$$\tilde{P}(\bar{A}, \bar{B}, A, B) = \overline{\tilde{P}(A, B, \bar{A}, \bar{B})}, \tag{B.19}$$

as well as identical equations for $\tilde{Q}$. Applying these relations to a monomial, $aA^pB^q\bar{A}^m\bar{B}^n$, we obtain $p+q-m-n-1=0$ and a real; $p+q+m+n = p+q+m+n \pm (p+q-m-n-1) = 2(p+q)-1 = 2(m+n)+1$, and all the monomials are of odd order. L_H also gives conditions on $\tilde{P}$ and $\tilde{Q}$:

$$\tilde{P}(sA, \delta_H A + sB, s\bar{A}, \delta_H\bar{A} + s\bar{B}) = s\tilde{P}(A, B, \bar{A}, \bar{B}), \tag{B.20}$$

$$\tilde{Q}(sA, \delta_H A + sB, s\bar{A}, \delta_H\bar{A} + s\bar{B}) = \delta_H\tilde{P}(A, B, \bar{A}, \bar{B}) + s\tilde{Q}(A, B, \bar{A}, \bar{B}). \tag{B.21}$$

The solution of these equations is

$$\begin{aligned}\tilde{P}(A, B, \bar{A}, \bar{B}) &= AP(|A|^2, \bar{A}B - A\bar{B}, \varepsilon),\\ \tilde{Q}(A, B, \bar{A}, \bar{B}) &= BP(|A|^2, \bar{A}B - A\bar{B}, \varepsilon) + AQ(|A|^2, \bar{A}B - A\bar{B}, \eta),\end{aligned} \tag{B.22}$$

i.e. Eq. (61).

Proof. Taking the derivatives of (B.20) and (B.21) with respect to δ_H, and putting $\delta_H = 0$, gives

$$A\partial_B\tilde{P} + \bar{A}\partial_{\bar{B}}\tilde{P} = 0, \qquad A\partial_B\tilde{Q} + \bar{A}\partial_{\bar{B}}\tilde{Q} = \tilde{P}. \tag{B.23}$$

Using new variables $x = A$, $y = \bar{A}$, $z = \bar{A}B - A\bar{B}$ and $t = B$, these equations reduce to

$$\partial_t\tilde{P} = 0, \qquad A\partial_t\tilde{Q} = \tilde{P}. \tag{B.24}$$

The solution for $\tilde{P}$ is $\tilde{P}(x, y, z, t) = \Phi(x, y, z) = xP(xy, z)$, using (B.19). The equation for $\tilde{Q}$ is $\partial_t\tilde{Q} = P(xy, z)$, whose solution is $\tilde{Q} = tP(xy, z) + \Psi(x, y, z)$. Again, using (B.18) for $\tilde{Q}$, $\Psi(x, y, z) = xQ(xy, z)$ and we arrive at (B.22). It can be verified by direct substitution that (B.22) satisfies (B.20) and (B.21). □

B.4. Normal form for $\mathcal{F}_2^{s_1} \oplus \mathcal{F}_2^{s_2}$

The normal form for $\mathcal{H}$ can be written as

$$A \mapsto s_1A + \tilde{P}(A, B, \bar{A}, \bar{B}), \qquad B \mapsto s_2B + \tilde{Q}(A, B, \bar{A}, \bar{B}) \tag{B.25}$$

and $\tilde{P}$ and $\tilde{Q}$ satisfy

$$\tilde{P}(\mathrm{e}^{\mathrm{i}\beta_1\alpha}A, \mathrm{e}^{\mathrm{i}\beta_2\alpha}B, \mathrm{e}^{-\mathrm{i}\beta_1\alpha}\bar{A}, \mathrm{e}^{-\mathrm{i}\beta_2\alpha}\bar{B}) = \mathrm{e}^{\mathrm{i}\beta_1\alpha}\tilde{P}(A, B, \bar{A}, \bar{B}), \tag{B.26}$$

$$\tilde{Q}(\mathrm{e}^{\mathrm{i}\beta_1\alpha}A, \mathrm{e}^{\mathrm{i}\beta_2\alpha}B, \mathrm{e}^{-\mathrm{i}\beta_1\alpha}\bar{A}, \mathrm{e}^{-\mathrm{i}\beta_2\alpha}\bar{B}) = \mathrm{e}^{\mathrm{i}\beta_2\alpha}\tilde{Q}(A, B, \bar{A}, \bar{B}), \tag{B.27}$$

$$\tilde{P}(\bar{A}, \bar{B}, A, B) = \overline{\tilde{P}(A, B, \bar{A}, \bar{B})}, \tag{B.28}$$

$$\tilde{Q}(\bar{A}, \bar{B}, A, B) = \overline{\tilde{Q}(A, B, \bar{A}, \bar{B})}, \tag{B.29}$$

$$\tilde{P}(s_1 A, s_2 B, s_1 \bar{A}, s_2 \bar{B}) = s_1 \tilde{P}(A, B, \bar{A}, \bar{B}), \tag{B.30}$$

$$\tilde{Q}(s_1 A, s_2 B, s_1 \bar{A}, s_2 \bar{B}) = s_2 \tilde{Q}(A, B, \bar{A}, \bar{B}). \tag{B.31}$$

Applying these relations to a monomial $aA^p B^q \bar{A}^m \bar{B}^n$ in $\tilde{P}$ and $\tilde{Q}$, we obtain

$$\begin{aligned} \tilde{P}: &\quad \beta_1(p-m-1) + \beta_2(q-n) = 0, \quad s_1^{p+m-1} s_2^{q+n} = 1, \\ \tilde{Q}: &\quad \beta_1(p-m) + \beta_2(q-n-1) = 0, \quad s_1^{p+m} s_2^{q+n-1} = 1 \end{aligned} \tag{B.32}$$

and a must be real. In the *non-resonant* case, where β_1/β_2 is irrational, the coefficients of β_1 and β_2 in the last equation must be zero, and the equations involving s_1 and s_2 are identically satisfied. $\tilde{P}$ and $\tilde{Q}$ are of the form:

$$\tilde{P}(A, B, \bar{A}, \bar{B}) = AP(|A|^2, |B|^2, \varepsilon), \qquad \tilde{Q}(A, B, \bar{A}, \bar{B}) = BQ(|A|^2, |B|^2, \eta)$$

which is (65).

Resonant case. The analysis is the same as in the non-resonant case up to Eq. (B.32). Now the ratio $\beta_1/\beta_2 = r/s$ is rational. Without loss of generality, we can take $0 < \beta_1 \leq \beta_2$, and the fraction r/s irreducible (i.e., $0 < r \leq s$). Eq. (B.32) for $\tilde{P}$ gives $r(p-m-1) = s(n-q)$, and as r/s is irreducible, $p = m+1+js$, $n = q+jr$, $j \in \mathbb{Z}$. The form of the monomial is $A(A^s \bar{B}^r)^j |A|^{2m} |B|^{2q}$, $j \in \mathbb{Z}$. The condition on s_1 and s_2 gives $(s_1^s s_2^r)^j = 1$, therefore j must be even when $s_1^s s_2^r = -1$. Treating $\tilde{Q}$ analogously, we arrive at

$$\begin{aligned} \tilde{P}(A, B, \bar{A}, \bar{B}) &= AP_1(|A|^2, |B|^2, \bar{A}^s B^r, A^s \bar{B}^r, \varepsilon) + \bar{A}^{s-1} B^r P_2(|A|^2, |B|^2, \bar{A}^s B^r, A^s \bar{B}^r, \eta), \\ \tilde{Q}(A, B, \bar{A}, \bar{B}) &= BQ_1(|A|^2, |B|^2, \bar{A}^s B^r, A^s \bar{B}^r, \lambda) + A^s \bar{B}^{r-1} Q_2(|A|^2, |B|^2, \bar{A}^s B^r, A^s \bar{B}^r, \rho), \end{aligned} \tag{B.33}$$

where ε, η, λ and ρ are real parameters, and when $s_1^s s_2^r = -1$, P_1 and Q_1 are even and P_2 and Q_2 are odd in their third and fourth arguments [$P_1(x_1, x_2, -x_3, -x_4) = P_1(x_1, x_2, x_3, x_4)$, and so on]. This gives the normal form (68).

References

[1] D. Barkley, R.D. Henderson, Three-dimensional Floquet stability analysis of the wake of a circular cylinder, J. Fluid Mech. 322 (1996) 215–241.
[2] D. Barkley, L.S. Tuckerman, M. Golubitsky, Bifurcation theory for three-dimensional flow in the wake of a circular cylinder, Phys. Rev. E 61 (2000) 5247–5252.
[3] H.M. Blackburn, J.M. Lopez, On three-dimensional Floquet instabilities of two-dimensional bluff body wakes, Phys. Fluids 15 (2003) L1–L4.
[4] H.M. Blackburn, J.M. Lopez, The onset of three-dimensional standing and modulated travelling waves in a periodically driven cavity flow, J. Fluid Mech. 497 (2003) 289–317.
[5] H.M. Blackburn, F. Marques, J.M. Lopez, On three-dimensional instabilities of two-dimensional flows with a Z_2 spatio-temporal symmetry, J. Fluid Mech., submitted for publication.
[6] P. Chossat, G. Iooss, The Couette–Taylor Problem, Springer, Berlin, 1994.
[7] P. Chossat, R. Lauterbach, Methods in Equivariant Bifurcations and Dynamical Systems, World Scientific, Singapore, 2000.
[8] M. Golubitsky, I. Stewart, The Symmetry Perspective: From Equilibrium to Chaos in Phase Space and Physical Space, Birkhäuser, Basel, 2002.
[9] M. Golubitsky, I. Stewart, D.G. Schaeffer, Singularities and Groups in Bifurcation Theory, vol. II, Springer, Berlin, 1988.
[10] G. Iooss, M. Adelmeyer, Topics in Bifurcation Theory and Applications, 2nd ed., World Scientific, Singapore, 1998.
[11] C.N. Jensen, M. Golubitsky, H. True, Symmetry, generic bifurcations, and mode interaction in nonlinear railway dynamics, Int. J. Bifurcat. Chaos 9 (1999) 1321–1331.
[12] Y.A. Kuznetsov, Elements of Applied Bifurcation Theory, 2nd ed., Springer, Berlin, 1998.
[13] J.S.W. Lamb, Local bifurcations in k-symmetric dynamical systems, Nonlinearity 9 (1996) 537–557.

[14] J.S.W. Lamb, I. Melbourne, Bifurcation from discrete rotating waves, Arch. Ration. Mech. Anal. 149 (1999) 229–270.
[15] J.E. Marsden, M. McCracken, The Hopf Bifurcation and Its Applications, vol. 19, Applied Mathematical Sciences, Springer, Berlin, 1976.
[16] J. Robichaux, S. Balachandar, S.P. Vanka, Three-dimensional Floquet instability of the wake of square cylinder, Phys. Fluids 11 (1999) 560–578.
[17] L. Russo, E. Mancusi, P.L. Maffettone, S. Crescitelli, Symmetry properties and bifurcation analysis of a class of periodically forced chemical reactors, Chem. Eng. Sci. 57 (2002) 5065–5082.
[18] J.W. Swift, K. Wiesenfeld, Suppression of period doubling in symmetric systems, Phys. Rev. Lett. 52 (1984) 705–708.
[19] M.J. Vogel, A.H. Hirsa, J.M. Lopez, Spatio-temporal dynamics of a periodically driven cavity flow, J. Fluid Mech. 478 (2003) 197–226.
[20] S. Wiggins, Introduction to Applied Nonlinear Dynamical Systems and Chaos, Springer, Berlin, 1990.